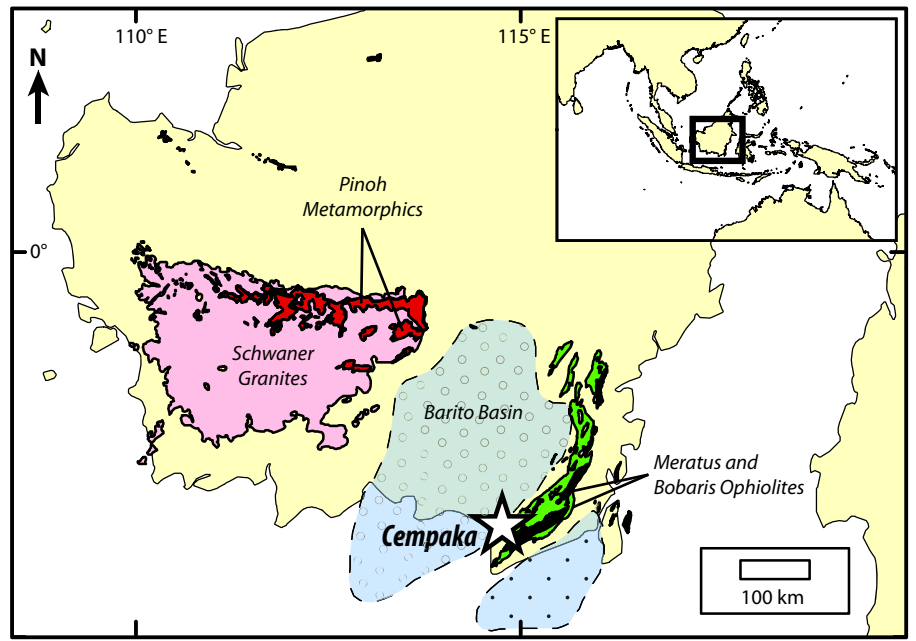

CEMPAKA ALLUVIAL DEPOSIT CONTAINS AT LEAST TWO SOURCES OF DIAMONDS WITH DIFFERENT TECTONIC HISTORY

GROUP A:

BROUGHT TO SURFACE BEFORE THE UPPER CRETACEOUS.

MANY SHOW FEATURES SUCH AS RADIATION BURNS AND HAVE BEEN REWORKED SEVERAL TIMES.

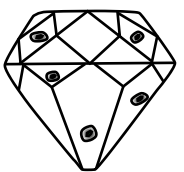

GROUP B:

ROUNDED DIAMONDS, BUT COULD NOT HAVE BEEN TRANSPORTED LONG DISTANCES AS THEY SHOW SHARP RESORPTION TEXTURES ON THE GRAIN SURFACE.

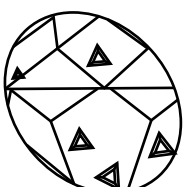

The provenance of Borneo's enigmatic alluvial diamonds: a case study from Cempaka, SE Kalimantan

L. T. White[1], I. Graham[2], D. Tanner[1], R. Hall[1], R. A. Armstrong[3], G. Yaxley[3], L. Barron[2,4], L. Spencer[5] and T. M. van Leeuwen[6]

1. Southeast Asia Research Group, Department of Earth Sciences, Royal Holloway University of London, Egham, Surrey, TW20 0EX, UK
2. School of Biological Earth and Environmental Sciences, University of New South Wales, Sydney, NSW, 2052, Australia
3. Research School of Earth Sciences, The Australian National University, Canberra, 0200, Australia
4. Geoscience, Australian Museum, Sydney, NSW, 2010, Australia
5. Consultant Geologist, St Huberts Island, NSW, Australia
6. Jl. H. Naim IIIB No. 8, Jakarta, 12150, Indonesia

Keywords: Kalimantan, exploration, provenance, detrital, diamond, zircon, geochronology

ABSTRACT

Gem-quality diamonds have been found in several alluvial deposits across central and southern Borneo. Borneo has been a known source of diamonds for centuries, but the location of their primary igneous source remains enigmatic. Many geological models have been proposed to explain their distribution, including: the diamonds were derived from a local diatreme; they were brought to the surface through ophiolite obduction or exhumation of UHP metamorphic rocks; they were transported long distances southward via major Asian river systems; or, they were transported from the Australian continent before Borneo was rifted from its northwestern margin in the Late Jurassic. To assess these models, we conducted a study of the provenance of heavy minerals from Kalimantan's Cempaka alluvial diamond deposit. This involved collecting U-Pb isotopic data, fission track and trace element geochemistry of zircon as well as major element geochemical data of spinels and morphological descriptions of zircon and diamond. The results indicate that the Cempaka diamonds were likely derived from at least two sources, one which was relatively local and/or involved little reworking, and the other more distal which records several periods of reworking. The distal diamond source is interpreted to be diamond-bearing pipes that intruded the basement of a block that: (1) rifted from northwest Australia (East Java or SW Borneo) and the diamonds were recycled into its sedimentary cover, or: (2) were emplaced elsewhere (e.g. NW Australia) and transported to a block (e.g. East Java or SW Borneo). Both of these scenarios require the diamonds to be transported with the block when it rifted from NW Australia in the Late Jurassic. The local source could be diamondiferous diatremes associated with eroded Miocene high-K alkaline intrusions north of the Barito Basin, which would indicate that the lithosphere beneath

50 SW Borneo is thick (~150 km or greater). The 'local' diamonds could also be
51 associated with ophiolitic rocks that are exposed in the nearby Meratus Mountains.
52
53 **1. Introduction**
54 The island of Borneo hosts numerous diamond-bearing alluvial deposits that are
55 found in four separate districts in Kalimantan (Krol, 1922; Koolhoven, 1935; van
56 Bemmelen, 1949; Sigit et al., 1969; Bergman et al., 1987; Smith et al., 2009) (Figure
57 1a). They occur in Upper Cretaceous to Recent rocks and sediments. These include
58 clastic sedimentary rocks of the Upper Cretaceous to Lower Paleogene Manunggul
59 Formation, which is found in the Meratus Mountains, as well as in Pleistocene
60 fanglomerates, Holocene alluvials and Recent alluvial conglomerates and river
61 terraces (Figure 1b) (Koolhoven, 1935; van Bemmelen, 1949; Spencer et al., 1988;
62 Lennie, 1997; Parkinson et al., 1998).
63
64 The earliest studies of Kalimantan's diamonds concluded that they were sourced from
65 kimberlite pipes associated with the ultrabasic rocks of the Bobaris Ophiolite (Figure
66 1a) (Krol, 1919, 1922; van Bemmelen, 1949; Seavoy, 1975). However, later
67 investigations showed that the rocks that were originally thought to be
68 diamondiferous peridotite (referred to as the "Pamili Breccia" or "Pamali Breccia")
69 were actually sedimentary in nature and composed of brecciated material derived
70 from the underlying Bobaris Ophiolite (Figure 1a) (Bergman et al., 1987; Burgath and
71 Mohr, 1991). This realization and subsequent mineralogical, petrological and isotopic
72 studies of Kalimantan's diamonds suggested an alternative origin: that they were
73 sourced from the sub-continental lithospheric mantle and transported to the surface
74 via kimberlite or lamproite pipes (e.g. Figure 2) (Smith et al., 2009) or derived from

distant sources, possibly involving multiple sedimentary recycling episodes. Whereas ultrapotassic alkaline intrusives such as kajanite and minette intrusions occur in several locations in West, Central and East Kalimantan (Wagner, 1986; Bergman et al., 1987, 1988; van Leeuwen, 2014) (Figure 1a), no indications of true lamproite or kimberlites have been found to date, let alone a diamond-bearing pipe or dyke. This does not mean that a primary igneous source does not exist on Borneo as it could simply reflect: (1) the difficulty of finding a relatively small intrusion in a large, intensely forested tropical island, and/or (2) the difficulty of preserving diamond-bearing primary source rocks in a region that experiences significant rainfall and weathers rapidly. The widespread distribution of chromite-bearing ultramafic rocks as well as abundant chromite and chromian-spinel bearing sediments in the drainage system mean that commonly used exploration techniques that focus on characterizing accessory phases of kimberlites and lamproites have been unsuccessful in this region.

The inability to find a local primary diamondiferous source has led to a number of other geological models to explain Kalimantan's diamonds. These include: (1) the diamonds were associated with ultramafic rocks that were obducted as an ophiolite (Nixon and Bergman, 1987); (2) the diamonds formed in a subduction zone setting and were brought to the surface in a process that did not involve a kimberlite/lamproite intrusion (Barron et al., 2008a); (3) the diamonds were transported a great distance, via large river systems that drained the Sibumasu Terrane before SW Borneo rifted from Indochina (Griffin et al., 2001) or (4) the diamonds were transported via large river systems from northwestern Australia before the SW Borneo block rifted from Gondwana in the late Jurassic (Hall, 2012; Hall and Sevastjanova, 2012; Metcalfe, 1996, 2011, 2013). In order to test such models, and

models that envisage a direct link between Borneo and the primary source(s) of its diamonds (e.g. van Leeuwen, 2014), we conducted a study of the provenance of heavy minerals from Kalimantan's Cempaka alluvial diamond deposit. Note, that the heavy minerals found in this deposit probably represent a mixture of heavy mineral species derived from multiple sources, and these sources likely differ from the primary source of the diamonds.

After 1987, work on the diamonds of the Cempaka region includes Spencer et al. (1988), Sun et al. (2005) and Smith et al. (2009). Spencer et al. (1988) report the discovery, testing and initial development of the Cempaka alluvial deposit, whereas Sun et al. (2005) and Smith et al. (2009) describe the morphology and genesis of present-day alluvial diamonds from Kalimantan. Sun et al. (2005) purchased 14 locally sourced gem-quality diamonds (ranging in size from 0.03 to 1.82 carats) for their study, while Smith et al. (2009) obtained 654 diamonds from South Kalimantan (with no precise locality details) from Rio Tinto Exploration. Thus, the research we present on diamonds in this paper represent the only suite obtained in situ from their alluvial host sediments.

Insert Figures 1 and 2

2. Tectonic history of Borneo during the Mesozoic

Before discussing the details of the possible provenance of the Cempaka alluvial deposit, it is useful to provide some background information on the tectonic evolution of Borneo in the Mesozoic. This is because the majority of geological models that

125 have been proposed to explain the primary source of Borneo's diamonds are large-
126 scale tectonic models and we refer to various terranes and their tectonic history
127 throughout the paper. The Mesozoic tectonic history is particularly important as the
128 oldest bearing diamondiferous sediments are the Upper Cretaceous Manunggal
129 Formation, meaning that at least some of the diamonds were brought to the surface,
130 eroded and re-deposited before the Late Cretaceous. In the Early Cretaceous, SW
131 Borneo had rifted from northwestern Australia, but had not yet accreted to Sundaland
132 (Hall, 2012) (Figure 3).
133
134 The continental crust of SE Asia has largely grown due to the amalgamation of
135 various crustal fragments that were rifted from Gondwana and were later juxtaposed
136 with rocks from Asia/Cathaysia as well as volcanic arc and ophiolitic rocks between
137 the Paleozoic and Early Cenozoic (e.g. Metcalfe, 1996, 2011, 2013; Hall, 2012). This
138 region of amalgamated continental crust marks the southernmost part of the Eurasian
139 plate and is commonly called "Sundaland" (Figure 4). Westernmost Sundaland is
140 composed of the Indochina-East Malaya, Sibumasu, West Burma and West Sumatra
141 blocks (Figure 4). These amalgamated with the North and South China blocks during
142 the Paleozoic to Triassic (Metcalfe, 1996, 2011, 2013; Hall, 2012).
143
144 Sundaland continued to grow during the Early to early Late Cretaceous with the
145 addition of the SW Borneo, East-Java West Sulawesi and Sabah-NW Sulawesi blocks
146 (Figure 4). These blocks were originally connected to Gondwana (western Australia),
147 but were torn from the supercontinent in the Late Jurassic (Metcalfe, 1996, 2011,
148 2013; Hall, 2012; Hall and Sevastjanova, 2012). The Cenozoic Cempaka alluvial
149 deposit, which is the focus of this paper, is found at the northeastern boundary of the

SW Borneo Block and the edge of the Meratus Suture Zone, which represents the Cretaceous tectonic boundary between the SW Borneo Block and the East-Java-West Sulawesi Block as defined by Hall (2012) (Figure 4).

Insert Figures 3 and 4

Much of Borneo and Sundaland is considered to have been emergent during the Jurassic and Cretaceous. Northern/northwestern Borneo however, was an active continental margin until early in the Late Cretaceous and was dominated by deep-water sedimentation (Hall, 2012, 2014). After about 80 Ma most of Sundaland was emergent (Hall, 2014). Volcanism and deformation phases associated with plate convergence and collision also mean that parts of Borneo (e.g. the Schwaner Mountains region) were likely to have been mountainous after 80 Ma (Clements et al., 2011; Hall, 2013; Davies et al., 2014). A terrestrial setting is supported by the development of a regional unconformity between the Cretaceous and Eocene (Clements et al., 2011), the presence of Laurasian conifer pollen in Late Cretaceous to Middle Eocene Sarawak sandstones (Muller, 1968), Cretaceous granitoids (Davies et al., 2014), and a predominance of Upper Cretaceous to Middle Eocene terrestrial sandstones in Sarawak and NW Kalimantan (Hall, 2013). A mountain chain also likely existed along the suture zone between Borneo and East Java from about 80 Ma, with this connection being marked by the now submerged Karimunjawa Arch (e.g. Hamilton, 1979; Smyth et al., 2007; Granath et al., 2011). The deep water sedimentation north of Borneo during this time combined with the high topographic relief of central Borneo means that that there were significant barriers to the transport of (diamond-bearing) sediments to, and within, Borneo.

175

176 **3. The Cempaka Deposit**

177 The Cempaka diamond deposit is located in SE Kalimantan (3°30'S, 114°45'E)
178 (Figure 1). Following decades of placer mining by local residents, it is the only
179 diamond deposit in Kalimantan that has been mined on a commercial scale, namely
180 by BDI Mining and other companies from 2002 to 2009 (van Leeuwen, 2014). The
181 earliest facies in the Cempaka area are Upper Cenozoic fanglomerates. These are
182 extensively laterized in areas of elevated topography and podsolised in areas below
183 the water table. The fanglomerates have been incised and eroded and subsequently
184 deposited into palaeochannels that are concealed beneath present-day swamps. The
185 palaeochannel sediments represent the last phase of alluvial reworking. These contain
186 the highest in-situ diamond grades and were subject to mining operations. The
187 diamondiferous fanglomerates and palaeochannel sediments were deposited at the
188 base of the Meratus Mountains (Figure 1). These fanglomerates overlie Cenozoic
189 sedimentary units within the Barito Basin, which in turn overlie Upper Jurassic to
190 Cretaceous metasediments, metavolcanics and granitic rocks (e.g. the Upper
191 Cretaceous to Paleogene Manunggal Formation from the Meratus Mountains, the
192 Schwaner Granitoids and the Pinoh Metamorphics) (Katili, 1978; Spencer et al.,
193 1988; Guntoro, 1999; Witts et al., 2011, 2012; Graham et al., 2014). The
194 conglomerates of the Manunggal Formation are also diamondiferous, so it is likely
195 that the younger alluvial deposits, such as Cempaka, were derived (at least in part)
196 from reworking of these older sedimentary rocks (Spencer et al., 1988).

197

198 The Cempaka placer also hosts PGE minerals and gold (Graham et al., 2014), which
199 not only constitute valuable by-products, but are also useful provenance indicators of

200 the source of the sediment. For instance, the gold in the Cempaka deposit is
201 characteristic of gold generated in an epithermal deposit and was transported more
202 than 10 km and/or reworked several times (Graham et al., 2014). It is likely that the
203 gold was sourced from one of the epithermal gold deposits from central Kalimantan
204 (e.g. van Leeuwen et al., 1990; van Leeuwen, 1994; Davies et al., 2008). It is unlikely
205 that the gold is related to the PGE minerals, which, based on their chemical
206 composition, were found to be from two distinct sources, an ophiolite and an Ural-
207 Alaskan complex (i.e. sub-arc cumulate) (Graham et al., 2014). Some of the PGE
208 minerals may therefore have been sourced from the nearby Meratus and Bobaris
209 ophiolites (Hattori et al., 1992, 2004; Graham et al., 2014).
210
211 Heavy mineral concentrates from the Cempaka alluvium are dominated by chromite
212 with minor ilmenite. Other accessory minerals that are present include zircon,
213 corundum, magnetite, rutile, diaspore and very rare garnet. The rutile and diaspore
214 only occur as large heavy particles (centimeters in size), and are not found in the
215 sand-sized fractions of heavy mineral separates. They are however, used by local
216 explorers as indicators to the proximity of diamonds.
217
218 Garnet and chromite chemistry can be useful indicators of kimberlites and lamproites
219 (Fipke et al., 1989; Barnes and Roeder, 2001), however, no typical 'kimberlitic'
220 indicator minerals have ever been reported from Cempaka (Spencer et al., 1988).
221 Such data may be restricted to propriety datasets or may not have been collected
222 because the Cempaka deposit is located down-stream of the Meratus and Bobaris
223 ophiolites, leading to the assumption that most, if not all, of the chromite was sourced
224 from these ophiolites. However, as there are no reports of such data, we collected

major element analyses of spinels, morphological descriptions of diamonds and zircons; as well as U-Pb isotopic, fission-track and trace element data from detrital zircons of the Cempaka deposit to assess their provenance.

4. Methodology

4.1 Sample Processing

A heavy mineral separate containing diamond, zircon and chromite was obtained by L. Spencer from the processing plant operated by BDI Mining. This sample consisted of material derived from the <2mm sieve fraction from run of mine ore. The screened material was passed through spiral separators to produce a low-grade heavy mineral concentrate. The low-grade spiral concentrate was then passed onto a Wilfley Table to remove silicates and the heavy concentrates from this were dried and passed over an Eriez rare earth magnet to remove chromite and ilmenite. The non-magnetic fraction was passed over a Gemini Table to produce a gold concentrate. Fine diamonds and zircons were obtained by manual sorting of the Gemini Table tailings. A parcel of 100 diamonds, ranging in size from 0.1 to 0.3 carats was selected for detailed morphological investigations. In addition, we also present data on the particle size distribution of 8863 diamonds that were included in an early feasibility study of the Cempaka mine (Spencer and Watson, 2002).

Spinel and zircon grains were hand-picked and mounted in circular resin blocks that were hand polished to expose the mid-section of individual grains for geochronological and geochemical analyses. Additional zircons were hand-picked for fission-track analyses. The possibility of contamination was extremely unlikely as the

processing plant was new and only processed gravels from the Cempaka paleoalluvium at the time of sample collection preparation.

4.2 Geochemistry

4.2.1 Spinel Chemistry

Spinel grains were mounted in polished resin blocks and major element analyses of spinels were measured using WDS on a Jeol8100 Superprobe at University College London (UCL). Analyses were collected at an accelerating voltage of 15 kV, a beam diameter of 1μm and a beam current of 2.5 nA. The counting times for all elements were 20 seconds on the peak and 10 seconds each on the high and low backgrounds. The analyses were calibrated against standards of natural silicates, oxides and Specpure® metals, with the data corrected using a ZAF program. The standard BCR-2G (Rocholl, 1998) was independently measured at the beginning and end of the session, as well as between every twelve unknown analyses to assess beam stability. The ferric iron content of the spinels was calculated by stoichiometry.

4.2.2 Zircon Chemistry

Zircons were analysed by LA-ICP-MS using an Excimer UV laser (193 nm), a Helex sample introduction system (Eggins et al., 1998a) and an Agilent 7500 quadrupole mass spectrometer, at the Research School of Earth Sciences, Australian National University (ANU). The spot size selected was 40 or 70 μm. The laser pulsed at 5 Hz, delivering 80mJ per pulse.

Ablation under a mixed $He+H_2$ atmosphere provided material carried to the plasma in an Ar/He gas stream. The mass spectrometer was tuned to optimum sensitivity and to minimise production of interfering oxides species, with $^{232}Th^{16}O/^{232}Th$ routinely ≤ 0.5%. The analyses were performed in peak hopping mode with a dwell time of 0.05 sec/mass. For each analysis the gas blank was acquired for 30 seconds, the laser triggered, and the signal acquired for a further 50 seconds.

The analytical protocol followed that of Eggins et al. (1998b). The primary calibration standard was NIST-612 glass and secondary standards basaltic glass BCR-2G (Govindaraju et al., 1994) and zircon 91500 (Wiedenbeck et al., 1995) were routinely analysed as unknowns to check data quality. Batches of analyses of 8 "unknowns" (unknown zircons and secondary standards 91500 and BCR-2G) were bracketed by analyses of NIST-612 allowing monitoring of, and correction for instrumental drift. Data reduction used background corrected count rates as established by Longerich et al. (1996). ^{91}Zr was measured enabling use of ZrO_2 abundances calculated on $ZrSiO_4$ stoichiometry (67.22 wt% ZrO_2) as the internal reference element. Calibration values for NIST-612 used in the data reduction are those of Eggins (2003). A linear drift correction based on the analysis sequence and on the bracketing analyses of NIST-612, was applied to the count rate for each sample. Data for the unknown zircons, based on multiple analyses of BCR-2G indicate that analytical reproducibility was better than 2% and accuracy was better than 5% for most reported elements. Data for the secondary standard zircon 91500 provided further control. La contents in six of the analysed zircons and in all 91500 standard zircon analyses were below the lower limit of detection (LLD) of 0.002 ppm, but in remaining zircons La values slightly

298 exceeded the LLD. Reported values for all other elements in the analysed and 91500
299 standard zircons were well above LLDs.
300
301 *4.3 Zircon Geochronology*
302 U-Pb isotopic measurements were collected from the detrital zircons using a Sensitive
303 High Resolution Ion Microprobe (SHRIMP-RG) at the Research School of Earth
304 Sciences, ANU. The zircon grains were imaged with a cathodoluminescent (CL)
305 detector fitted to a scanning electron microscope at the Research School of Earth
306 Sciences prior to collecting any isotopic data. The CL imagery as well as reflected
307 and transmitted light microscopy were used to identify zircon cores and growth rims
308 that were suitable for dating. Standard zircon SL13 (U = 238 ppm; Th = 21 ppm;
309 Claoué-Long et al., 1995) was used to calibrate the U and Th concentrations and Pb/U
310 ratios were corrected for instrumental interelement fractionation using the ratios
311 measured on the standard zircon Temora 2 (416.8 ± 1.3 Ma; Black et al., 2004). One
312 analysis of a Temora zircon was analysed for every four analyses of unknowns. The
313 data have been reduced in a manner similar to that described by Williams (1998, and
314 references therein), using the SQUID 2 Excel macro of Ludwig (2009). The decay
315 constants recommended by the IUGS Subcomission on Geochronology (as given in
316 Steiger and Jäger, 1977) were used in age calculations. Uncertainties given for
317 individual U-Pb analyses (ratios and ages) are at the 1 sigma level. All age results that
318 are less than 800 Ma are reported using ^{207}Pb corrected ^{206}Pb/^{238}U ages, whereas ages
319 that are >800 Ma are reported using ^{204}Pb corrected ^{207}Pb/^{206}Pb ages.
320

4.4 Zircon Thermochronology

Fission-track thermochronological analyses were conducted on twenty zircon grains. Prior to analysis, the grains were subdivided into a >1 mm group of colourless rounded zircons and a <1 mm group of colourless euhedral zircons. Zircons greater than 1mm in size were first crushed into sub-mm fragments in order to make them suitable for analysis. We did not take multiple fragments from single grains for separate evaluation. The zircons were embedded in FEP Teflon sections, polished and etched in a molten KOH: NaOH eutectic mixture at ~ 220ºC (Gleadow et al., 1976) for over 39 hours (sub-mm grains) and 46 hours (+ mm grains) to reveal the fission tracks. The samples, along with low-U muscovite mica detector plates were irradiated at the Australian Atomic Energy Commission HIFAR research reactor, Lucas Heights, Sydney. The track counting was made using a Zeiss Axioplan microscope. The fission track ages were calculated using the zeta calibration method (Green, 1985) and a zeta factor of 87.7 ± 0.8 for dosimeter glass U3. The grain ages and errors incorporated Poissonian statistics and radial plot diagrams (Green, 1981; Galbraith, 1988, 1990).

5. Results

5.1 Spinel Morphology and Geochemistry

The spinel grains that were selected as part of this study are angular to sub-rounded grains that are ~0.5 – 1.0 mm in diameter. Eighty-nine major element analyses were collected from forty-four spinel grains (Supplementary Data Table 1). The grains showed no evidence of zonation on backscattered SEM images. Analyses were therefore collected from the center of each grain. The chemical data were used to

346 verify the provenance of spinels and to test if a potential lamproitic or kimberlitic
347 source was possible. We therefore compared our results with those in a global spinel
348 database (Barnes and Roeder, 2001). The majority of Cempaka spinels are chromium
349 spinels and plot within the 30th and 50th percentiles of the global 'ophiolite' field
350 (Figure 5) (Barnes and Roeder, 2001). This finding reflects the local sedimentary
351 input from (non-diamondiferous) ophiolites. This is not surprising as erosion and re-
352 deposition of material from the nearby Bobaris and Meratus ophiolites (Figure 1a)
353 were expected to dilute any spinels associated with a kimberlite or lamproite.
354
355 *Insert Figure 5*
356
357 The analyses that fall outside of the 30th and 50th percentiles (Figure 5) are not
358 anomalous and are within the range of the global spinel database (Barnes and Roeder,
359 2001). Although some of the chemical analyses of Cempaka spinels plot outside the
360 30th and 50th percentiles of the global ophiolite field and might be interpreted to be
361 derived from a kimberlitic or lamproitic source (Figure 5), such results also fall within
362 the total range of spinel chemistries from ophiolites. From these results, we concluded
363 that the spinel geochemical data do not provide definitive information as to the
364 possibility of a diamondiferous diatreme.
365
366 *5.2 Zircon Morphology, Geochronology, Thermochronology and Geochemistry*

367 5.2.1 U-Pb dating and zircon morphology

368 U-Pb isotopes from fifty-eight zircons from the Cempaka deposit were analyzed using
369 SHRIMP-RG (Supplementary Table 2). The majority of grains that were analyzed
370 were concordant (Figure 6) and two thirds of the concordant zircon grains crystallized

between 75 Ma and 110 Ma. The age results broadly correspond with the morphology of the zircons, as Cretaceous ages were obtained only from euhedral grains, outer growth rims or angular zircon grain fragments (Figure 7). The remaining analyses were Triassic or older (223 Ma, 314-319 Ma, 353-367 Ma, 402-414 Ma, 474 Ma, 521 Ma, 1135-1176 Ma, 1535 Ma and 2716 Ma). The Triassic and older analyses broadly correspond to the rounded, semi-rounded and angular zircon grains and cores (Figure 7), indicating that the older grains were derived from a more distal source and/or zircons that have undergone several phases of recycling.

Insert Figure 6

Insert Figure 7

The range of morphologies and textures from the Cempaka detrital zircons are best shown in secondary electron SEM images of non-polished grains (Figure 8). These include rounded and sub-rounded grains (Figure 8a-c) that are indicative of transport in a high-energy environment for some time. These also include euhedral angular grains (d-i), many of which preserve primary growth textures (Figure 8e-f), preserved mineral inclusions (Figure 8d) or zones where mineral inclusions have been chemically or mechanically removed (Figure 8g-i), all of which would not be preserved with prolonged transport in a high-energy environment.

Insert Figure 8

The U-Pb detrital zircon data that were collected as part of this study were compared with recently published detrital U-Pb age data from the Schwaner Granitoids, Pinoh Metamorphics and Barito Basin (Witts et al., 2011, 2012; Davies et al., 2014) as well as data from the Khorat Plateau Basin of eastern Thailand (Carter and Moss, 1999; Carter and Bristow, 2003) (Figure 9). All of the age results from samples that were collected within Borneo show a dominant age population between ~75 and 110 Ma and are broadly similar (Figure 9a-h). This Cretaceous age population does not exist in the zircons dated from the Khorat Plateau Basin (Figure 9i-j), and there are few similarities between these zircons and those obtained from the Borneo samples (Figure 9). This indicates that it is extremely unlikely that the Borneo sediments were derived from the same sources as those for the Khorat Basin.

We propose that Cretaceous zircons in the Cempaka alluvium are most likely to be sourced from the Schwaner Granitoids and Pinoh Metamorphics. This hypothesis is supported by: (1) ages reported from these granites and metamorphics (Davies et al., 2014); and (2) the angular morphology of zircon grains and rims that are younger than ~110 Ma indicates that these zircons have not been extensively reworked and/or transported from a distal source. It is also possible that these zircons could be sourced from much greater distances if they were derived from ash fall associated with explosive eruptions. However, since the Schwaner Mountain granitoids are the closest and largest area of zircon-rich material to the Cempaka deposit, and have very similar age populations, we consider them to be the most likely source of zircons. Cretaceous K-Ar ages are reported for igneous and metamorphic rocks in the Meratus Mountains and other nearby regions such as Java and SW Sulawesi (e.g. Bergman et al., 1996;

419 Hartano et al., 1999) but zircon-bearing rocks, such as granites, in these areas are
420 absent or uncommon.
421
422 Detailed characterization of the regional stratigraphy using a combination of
423 sedimentary logging, biostratigraphy and detrital U-Pb geochronology indicate that
424 the erosion of the Schwaner Granitoids and Pinoh Metamorphics occurred during the
425 Eocene to Miocene (Witts et al., 2011). The erosional products were redeposited in
426 the sedimentary units of the Barito Basin along with material from another southerly
427 source (Figure 1) (Witts et al., 2011). The southerly source of zircon was most likely
428 the Karimunjawa Arch (or equivalent area). This provided material that was originally
429 the sedimentary cover to the SW Borneo or East Java blocks and accounts for the
430 Phanerozoic and Precambrian zircons within the Barito Basin (Witts et al. 2011).
431 Reworking and re-deposition of the Barito Basin sediments can therefore explain the
432 Phanerozoic and Precambrian zircons in the Cempaka alluvium. The majority of these
433 grains are rounded to sub-angular (Figures 7-8), indicating transport from distal
434 sources and/or multiple sedimentary cycles. We therefore interpret the pre-Cretaceous
435 zircons to represent reworked detrital zircons from the Barito Basin. The Cempaka
436 alluvium may also include zircons reworked from the Upper Cretaceous to Paleogene
437 Manunngal Formation and potentially the Pinoh Metamorphics. However, this is
438 more speculative since no detrital zircon age data are available for the former, and
439 only one sample of quartzite from the Pinoh Metamorphics yielded pre-Cretaceous
440 zircons (Davies et al., 2014).
441
442 *Insert Figure 9*
443

444 5.2.2 Zircon fission-track ages

445 Fission track ages were obtained from twenty zircon grains. The counting statistics, U
446 contents and age analyses of the zircons are presented in Supplementary File 3. The
447 zircons dated by fission track (FT) were subdivided into two groups according to their
448 size prior to analysis. The ten grains that were >1 mm in diameter yielded a well-
449 defined fission-track age of 129.6 ± 7.3 Ma (MSWD = 1.6), however, the sub-mm
450 zircons yielded a mixture of Cretaceous to Pliocene ages. The results are best
451 displayed on a relative probability-frequency plot that shows the relative proportion of
452 ages obtained from the two size fractions (Figure 10). This plot shows that there are
453 three dominant age populations where the oldest population corresponds to the >1mm
454 zircons, whereas the two younger populations correspond to the <1mm zircons. A
455 quantitative value for each of these populations was calculated using the 'unmix age'
456 algorithm (Sambridge and Compston, 1994) within Isoplot 2.0 (Ludwig, 2003). The
457 youngest population is 3.5 ± 1.8 Ma (2σ) and represents 10% of the population. The
458 Late Cretaceous age peak is 80.2 ± 6.7 Ma (2σ) and represents 37% of the population.
459 The oldest peak was calculated to be 122.4 ± 17 Ma (2σ) and represents 53% of the
460 population. Several older FT ages were obtained (171, 175, 178 and 190 Ma), all of
461 which have very large one-sigma uncertainties (20-50 Ma). The large uncertainties
462 associated with these older ages mean that they are within error of the ~122 Ma age
463 population.

464

465 The Late Cretaceous FT ages however, likely reflect the cooling history of the zircons
466 after a period of Cretaceous magmatism and/or metamorphism led to the annealing of
467 fission-tracks in pre-Cretaceous zircons across the region. Considering that the <1mm
468 zircons are primarily angular euhedral grains, they were likely derived from a nearby

source. We suspect the Schwaner Granites and Pinoh Metamorphics could represent possible sources for the Late Cretaceous zircon FT ages, especially considering that the 80.2 ± 6.7 Ma age population is within error of 76 ± 8.7 Ma apatite and zircon fission track ages obtained from an in-situ sample of the Batuan Pluton of the Schwaner Mountains (Sumartadipura, 1976). However, as mentioned earlier, it is also possible that the Cretaceous zircons were sourced from ash that was ejected from proximal or more distal explosive volcanic eruptions, with zircons being distributed (and later recycled) into surface deposits after they fell back to the Earth's surface.

If these zircons are from the mid-late Cretaceous Schwaner Granites or Pinoh Metamorphics, the FT results indicate that the source of Cretaceous zircons was uplifted relatively soon after zircon crystallization (i.e. to ensure the zircon passed its 240°C ± 30° closure temperature for fission-track development; Bernet and Garver, 2005). We suspect that the Pliocene zircon FT ages could reflect the uplift and cooling of Miocene or older intrusives or volcanics, or alternatively, represent zircons associated with the eruption or erosion of Pliocene volcanics in central Kalimantan (e.g. Soeria-Atmadja et al., 1999).

Insert Figure 10

5.2.3 Zircon geochemistry

Trace element geochemical data were obtained from forty-five zircons from the Cempaka alluvium (Supplementary Data 4). These zircons generally have <100 ppm Ce, Sm, Eu, Gd, Sr, Ho, Lu, and Nb, <400 ppm Dy, Er, Th and U as well as concentrations of Y between 100 ppm and 2300 ppm (Supplementary Data 4).

494

495 The trace element geochemistry of zircons has been used to infer information about
496 their provenance, particularly in the search of kimberlites (e.g. Belousova et al.,
497 2002). We therefore compared the range of trace element compositions of the
498 Cempaka detrital zircons with those of zircons from igneous rocks (Belousova et al.,
499 2002) (Figure 11a-e). This shows that there is a striking similarity between the
500 Cempaka zircons and those of lamproites and basalts, particularly the Y content.
501 These data also show that the Cempaka zircons have much higher concentrations of
502 REE, Th and Y as well as higher Nb/Ta and Zr/Hf ratios than the average
503 compositions of zircons from kimberlites (Belousova et al., 2002). The trace element
504 compositions of the Cempaka zircons are also generally depleted relative to the range
505 of composition of zircons from granitoids, however zircons from granitoids do span a
506 large range of compositions (Belousova et al., 2002) (Figure 11a-e and
507 Supplementary Data Table 4). Therefore, we do not consider these comparisons of
508 zircon trace element data to be particularly useful provenance indicators.

509

510 *Insert Figure 11*

511

512 Such comparisons of zircon trace element geochemistry are also dependent on
513 whether the data presented by Belousova et al. (2002) are representative of the
514 proposed lithologies. Belousova et al. (2002) state that the lamproitic zircons that
515 were analysed in their study represent xenocrysts, sourced from granitic and syenitic
516 host rocks. This means that the striking similarity between the detrital Cempaka
517 zircons with 'lamproitic zircons' is fortuitous, and that the trace element data reflects
518 a granitic or syenitic source, rather than a lamproite. In addition, zircon is very rare in

519 lamproite, with exception of the Smoky Butte lamproite. This is thought to be due to
520 the higher degree of polymerization of lamproite melts (Mitchell and Bergman, 1991).
521 Considering these points alongside the U-Pb data obtained in this study and our
522 knowledge of the regional geology, we propose that trace element data obtained from
523 the Cempaka zircons represents a mixture of igneous and metamorphic zircons that
524 were probably sourced from the erosion of the Schwaner Granites and Pinoh
525 Metamorphics as well as basaltic and ultramafic rocks in the Meratus Mountains and
526 igneous rocks from the Kelian region. There is some indication of this mixture of
527 sources in the trace element data (e.g. Ce vs. Hf) (Figure 11f). This is particularly
528 apparent when we consider the trace element data alongside other factors such as
529 grain size and the results obtained from the FT study (e.g. Figure 11f), which clearly
530 indicates that the zircons that yielded Mio-Pliocene FT ages have a different
531 composition to the majority of the other zircons that were analysed.
532
533 *5.3 Diamond Morphology*
534 Cempaka diamonds range in size from micro-diamonds (<0.1 mm) through to a
535 maximum of 66.2 carats. Of the 100 macro-sized diamonds that were examined in this
536 study, forty-three percent are colourless, indicating they have low nitrogen
537 concentrations, whereas another forty percent of the diamonds are yellow/brown,
538 indicating they have relatively high nitrogen concentrations. Both Spencer et al.
539 (1988) and Sun et al. (2005) also found that the diamonds were yellow, brown or
540 colourless, whereas Smith et al. (2009) found that yellow diamonds were less
541 common. Of particular note is that Spencer et al. (1988) also recorded green diamonds
542 and a 3.5-carat cobalt blue diamond was recovered during diamond mining operations
543 at Cempaka in 2006. Importantly, also examined was a range of semi-opaque black

544 diamonds and ballas. Spencer et al. (1988) noted that ballas was rare in their trial bulk
545 sample, but neither ballas, nor opaque black diamonds were noted in other studies of
546 SE Kalimantan diamonds (Sun et al., 2005; Smith et al., 2009). Also of note was the
547 discovery of a large carbonado at Cempaka (e.g. van Leeuwen 2014).
548
549 In terms of morphology, the diamond population that we studied is dominated by
550 variously modified dodecahedron, tetrahexahedron, octahedron and macles (Figure
551 12) while cubes are rare. This is in good agreement with the previous findings of
552 Spencer et al. (1988), Sun et al. (2005) and Smith et al. (2009). In contrast, the semi-
553 opaque to ballas diamonds comprise various forms of octahedron, cubo-octahedron or
554 rough-textured ovoid-shaped grains (Figure 13). In this population, the black platy
555 inclusions within the semi-opaque diamonds are graphite (Figure 13).
556
557 Other clearly distinguishable morphological features include:
558 • Seventy-five percent of the diamonds show evidence of plastic deformation
559 during growth such as fine plastic deformation lamellae (Figure 12a), cross
560 striae and volume strain birefringence. These were also found by Smith et al.,
561 (2009).
562 • Fifty percent of the diamonds are composite grains that show evidence of
563 growth zoning, with outer 'rims' with abundant mineral inclusions and inner
564 'cores' with very few to no mineral inclusions (Figure 14).
565 • Twenty-six percent of the diamonds show resorption features (Figure 15a)
566 • Fifty percent of the diamonds have radiation damage (Figures 12c and 15b).
567 • Twenty percent of the diamonds have percussion marks while twenty eight
568 percent have rhombic cracking.

- Some seventy-five per cent of the studied diamonds show at least some strain birefringence.
- Diamonds with well-developed sharp hexagonal-shaped negative crystal indentations are uncommon (Figure 15a)
- Micro-discs are relatively common on the surface of many of the gem-quality diamonds and are up to 0.2 mm in diameter (Figure 15c)
- As found by Smith et al. (2009), octahedral zonation is seen in polarized light for some of the diamonds (Figure 15d).
- As noted previously by Smith et al. (2009), a high proportion of the diamonds have smooth shiny polished surfaces (Figures 12b and 15a).

Insert Figures 12-15

The morphology, surface features and occurrence of ballas indicates that there are at least two different sources of diamonds in the Cempaka alluvial deposit. Some 26% of the observed diamonds have sharp resorption features and planar deformation features while 74% lack these characteristics. Such features include micro-discs (Figure 15a), fine planar deformation lamellae (Figures 12a and 12c) and euhedral negative crystal indents (Figure 15a). Similar surface features including trigons and cross-hatched lamination lines were reported by Sun et al. (2005). Additionally, only 20% of the diamonds studied have percussion marks, while Sun et al. (2005) reported percussion marks to be abundant in the diamonds that they studied. Alluvial transport surface features described by Smith et al. (2009) included rhombic cracks, abraded points and fretted edges. The combination of diamonds with sharp angular well-defined surface features with diamonds lacking such features suggests that at least

two populations are present within the alluvial deposit, one from a distal and/or reworked alluvial source and one from a more proximal source.

In terms of the rhombic cracking, in this study it was found to penetrate some 200 microns into the diamond surface and thus represents activation of the [111] cleavage at or near the diamond's surface. In terms of distribution, rhombic cracking occurs on most diamond morphologies and only one of the diamonds with rhombic cracking was also found to show evidence of mechanical damage by alluvial transport. Although Smith et al. (2009) suggested that this texture was due to surficial transport, we instead suggest that this texture is due to elastic deformation up to the point of failure. Evidence for this explanation is that the texture occurs throughout the whole diamond, though sometimes it occurs in distinctive bands. The exact mechanism could be either: (1) regional stress during metamorphism of the surrounding country rock, or (2) local differential stress during rapid heating/cooling of the surrounding country rock. Although 50% of these diamonds also have brown radiation spots, only 10% of diamonds with radiation spots also have rhombic cracking. Thus, the diamonds with rhombic cracking may represent another distinctive source group.

Additional evidence for at least two sources of diamonds is provided by the occurrence of semi-opaque to opaque black diamonds with abundant graphite inclusions and subhedral to anhedral angular to well-rounded ballas (Figure 13). The semi-opaque varieties additionally contain brown outer radiation spots (Figure 13a). Barron et al. (2008) found that many of these ballas diamonds are composite diamonds (see below).

619 Four of the diamonds studied have a preserved green colour (Figure 14a), interpreted
620 to be due to radiation damage of the surface. Similar partial to complete green outer
621 surfaces on diamond have been previously described from the Timber Creek diatreme
622 in the Northern Territory, Australia (Kolff, 2010). Brown radiation damage is far
623 more common (Figures 12d and 14d) and occurs in 46% of the diamonds examined in
624 this study. These radiation 'spots' are relatively sharp and well-defined with equant to
625 rectangular shapes. The high abundance of diamonds with these radiation 'spots'
626 suggests that they have been buried within an alluvial package containing a relatively
627 high abundance of radioactive minerals such as zircon and/or monazite, or they were
628 exposed to uranium-bearing fluids within the sedimentary basin. Four of the
629 diamonds studied have both green and brown spots, indicating that they have been
630 involved in multiple alluvial cycles. Some diamonds contain up to 100 radiation
631 spots. Sun et al. (2005), Barron et al. (2008a) and Smith et al. (2009) also described
632 the common occurrence of brown and green spots within Kalimantan diamonds. The
633 green spots are ascribed to the diamonds having been in close proximity to radioactive
634 minerals for extended periods of time (Vance et al., 1973) while the brown spots
635 indicate exposure to alpha particle damage and temperatures of at least 550-600°C
636 (Vance et al., 1973; Bosshart, 1993). This implies that the diamonds with brown spots
637 were buried deep within a sedimentary package that was subsequently
638 metamorphosed under amphibolite facies conditions (Miyashiro, 1994). The fact that
639 almost half of the diamonds in this study contain obvious radiation damage while the
640 other half do not is again strongly suggestive of two sources for the Cempaka
641 diamonds. One population was deeply buried within a sedimentary package and
642 subsequently metamorphosed, and the other population, most likely younger, was not
643 subjected to such deep burial and radiation damage.

644

645 The composite diamonds (50% of the measured population) are also particularly
646 characteristic of the Cempaka deposit, though these were not mentioned by either Sun
647 et al. (2005) or Smith et al. (2009). These comprise a 'core' and 'rim' that consist of a
648 semi-opaque to opaque overcoat on resorbed octahedrons. We speculate that these
649 'cores' and 'rims' indicate that the diamonds entered the diamond stability field twice,
650 possibly due to upward and downward movement of the lithospheric root prior to the
651 diamonds being brought to the surface in a diatreme (e.g. Figure 2). When viewed
652 through normal light these diamonds appear to be opaque, when a "window" is cut
653 through the surface, the bulk of the diamond is transparent (Figures 14b-14d). The
654 outer overcoat comprises poorly defined 6-sided plates (Figure 14d). At the rim/core
655 interface are abundant trapped inclusions of quartz, chamosite, Cr-magnetite, Y-
656 xenotime, Y-churchite, and a KFeAlSi oxide glass. While the cores of these diamonds
657 are extremely hard (amongst the hardest known), the outer diamond rims are not and
658 would be destroyed after prolonged transport.

659

660 These data support the outcomes of an earlier study of diamonds from across
661 Kalimantan that indicated the diamonds could have been derived from up to four
662 different primary sources (Smith et al., 2009). These workers found that 68% of their
663 sample-set were peridotitic diamonds and 32% were eclogitic diamonds. They also
664 proposed that the diamonds resembled those that had been transported from the
665 subcontinental lithospheric mantle to the surface by a kimberlite or lamproite. It is
666 therefore likely that at least some of the diamonds from Cempaka (especially those
667 with sharp resorption features, fine planar deformation striae and sharp negative
668 crystal indents) were derived from a local source. This interpretation is further

supported by the multi-modal grain-size distribution of diamonds from the deposit (Figure 16). We would expect a uni-modal grain-size distribution if all of the Cempaka diamonds were obtained from the same source. Also, the grain size distribution data indicates that fine grained (<1mm) diamonds exist in the Cempaka alluvium. These are associated with fine-grained ballas. Together, these would not survive multiple episodes of sedimentary recycling and metamorphism, indicating that these diamonds and ballas were derived from a local source.

There are two possible local sources: (1) the diamonds were sourced from ophiolites or high-pressure metamorphic rocks (e.g. eclogite) in the nearby Meratus Mountains, or (2) the diamonds were sourced from local, yet undiscovered diamondiferous diatremes (potentially associated with a period of high-K alkaline intrusive activity, e.g. the ~8 Ma Linhaisai Minette; Bergman et al., 1988). We discuss these models in more detail in the following section, along with hypotheses about the source of the more distal/reworked diamonds.

Insert Figure 16

6. Discussion

6.1 Assessing potential sources of Kalimantan's diamonds

6.1.1 Local Diatremes

Exploration companies have been searching for diamondiferous diatremes in Borneo for decades (van Leeuwen, 2014). Despite considerable effort none have been found to date. However, there have been some discoveries of ultrapotassic alkaline

694 intrusions, such as the ~8 Ma Linhaisai Minette (Figure 1a) (Bergman et al., 1988).
695 The Linhaisai Minette does not contain diamonds, but is significant in that it indicates
696 that the tectonic regime at the time was conducive for the emplacement of
697 ultrapotassic alkaline intrusions. Others have suggested Neogene potassic and ultra-
698 potassic volcanic rocks that occur in various parts of Kalimantan could be a potential
699 primary source of Neogene or younger alluvial diamonds (Simanjuntak and
700 Simanjuntak 2000). Young high-potassic alkaline intrusions associated with this
701 phase of magmatism in Borneo could be a candidate primary source for ~26% of the
702 Cempaka diamonds with resorption features indicating that these were likely derived
703 from a proximal source. The major challenge however is in finding relatively small
704 intrusions in Borneo's heavily forested tropical rainforests. Exploration via mapping
705 and stream sampling is particularly difficult with no guarantee of success. In addition,
706 there is also a lack of high-resolution magnetic data collected with a line spacing
707 conducive to finding weakly magnetic bodies of low surface area amongst strongly
708 magnetic peridotites and their erosional products.
709
710 Other proximal, non-traditional diamond sources might also explain some of the
711 diamonds in Borneo. For instance, recent work in Kamchatka has shown that there are
712 micro-diamonds trapped within pumice ejected from arc volcanoes (Gordeev et al.,
713 2014; Karpov et al., 2014). No macrodiamonds such as those found at Cempaka have
714 been recovered from the Kamchatka volcanics, but if future work is able to identify
715 macrodiamonds in these eruptive sources, then these could be a possible explanation
716 for some of the Cempaka diamonds.
717

718 However, a relatively young local source only explains some of the diamonds, as our
719 results also indicate that ~74% of the Cempaka diamonds do not have resorption
720 features and are characterized by radiation burns and percussion marks, so there must
721 be another source. This other source is probably older than Late Cretaceous as some
722 of Kalimantan's diamonds are found in Upper Cretaceous conglomerates (e.g. the
723 basal sequences of the Manunggul Formation (Katili, 1978; Sikumbang, 1990;
724 Spencer et al., 1998; Guntoro, 1999).
725

726 6.1.2 Ophiolitic Source

727 A potential primary ophiolitic source for Borneo's diamonds was proposed by Nixon
728 and Bergman (1987) and Bergman et al. (1987). This model was proposed after the
729 realization that the Pamili Breccia could not be a primary diamond source (e.g.
730 Bergman et al., 1987), and because some streams in SE Kalimantan are more
731 diamondiferous where they flow over the base of an Upper Cretaceous sedimentary-
732 volcanic unit that unconformably overlies ophiolitic rocks (e.g. the Pamali Breccia).
733 This model was also proposed because of the proximity of the Cempaka alluvial
734 deposit to the Meratus and Bobaris ophiolites (Figure 1a) and because there are
735 diamonds in the drainages emanating from both the west and southeast of Cempaka,
736 with the Meratus Mountains representing an obvious source. This proximity is
737 reflected in the large proportion of chromium-spinels and PGE minerals found within
738 the Cempaka gravels (Zientek et al., 1992; Graham et al., 2014; this study). There are
739 also intramontane basins containing diamondiferous fanglomeratic sediments derived
740 from the erosion of the Manunggal Formation. A Meratus Mountains/ophiolitic
741 source is also supported by the recent discovery of 5 microdiamonds (600-800 μm in
742 diameter) from a stream sediment sample collected within an ultramafic cumulate

743 complex on Sebuku Island, offshore SE Borneo (Swamidharma et al., 2015). These
744 diamonds apparently show no signs of abrasion and the ophiolitic rocks that are
745 exposed in the area are not covered by Cenzoic sedimentary rocks (Swamidharma et
746 al., 2015).
747
748 Ophiolitic peridotites and podiform chromites are now widely recognized as a source
749 of microdiamonds, particularly in China, Russia and Myanmar (e.g. Yang et al.,
750 2014). These microdiamonds are typically 0.2-0.5 mm diameter inclusions within
751 magnesiochromitite grains, are yellowish-green and have very distinctive light carbon
752 isotopic compositions (Yang et al., 2014). They also commonly contain inclusions of
753 Ni-Mn-Co alloy and this can be used to distinguish them from kimberlitic and
754 metamorphic diamonds. We have not conducted these analyses on the Cempaka
755 diamonds, but we are reasonably confident that an ophiolite model cannot account for
756 the macrodiamonds reported from the Cempaka deposit.
757
758 Ophiolitic diamonds are considered to form due to the recycling of continental crust
759 via subduction into the mantle transition zone, with water, carbon dioxide and other
760 fluids being released from these subducted rocks and mixing with highly reduced
761 mantle fluids to produce diamonds that can become encapsulated in chromite if the
762 melts/fluids rise above depths of ~300km (Robinson et al., 2011). However, the
763 mechanism of transportation of the diamond-within-chromite to the surface is
764 unresolved. One idea is that transport is driven by plumes or superplumes (Yang et
765 al., 2014). Another possibility may be rapid exhumation of the diamond-bearing-
766 chromite upper mantle rocks during crustal extension (e.g. Pownall et al., 2013,
767 2014), potentially followed by a phase of thrusting after a tectonic mode switch (e.g.

768 Lister and Forster, 2009). This tectonic scenario would not sensu-stricto equate to
769 ophiolite obduction, and if correct would mean that the Meratus and Bobaris
770 ophiolites represent peridotites rapidly exhumed from deep in the upper mantle. This
771 is a possibility, but requires further investigation.
772
773
774 6.1.3 Subduction Source
775 Borneo's diamonds have also been said to form during UHP metamorphism within a
776 subduction zone and later exhumed due to a process that did not involve a kimberlite
777 intrusion (e.g. Figure 17) (Barron et al., 2008a). This model was proposed to explain
778 similarities between the Cempaka diamonds and alluvial diamond deposits in eastern
779 Australia (the Copeton and Bingara deposits) (Barron et al., 2008a,b). Diamonds from
780 these deposits share: (1) similar nitrogen characteristics, (2) second order Raman
781 spectroscopy peaks that are suppressed relative to the spectra obtained from cratonic
782 diamonds, and (3) similar internal pressure estimates from inclusions (7.5 - 19 kb)
783 (Barron et al., 2008a). Some of the Australian alluvial diamonds are also deformed
784 and were also deposited near an uplifted and deformed continental volcanic arc
785 (Scheibner and Basden, 1998; Barron et al., 2008a,b). Borneo's diamond deposits also
786 contain significant amounts of igneous and metamorphic clasts and minerals (e.g.
787 magnetite, muscovite and gold). Some workers have interpreted this to mean that the
788 diamonds were derived from an igneous or metamorphic source (Burgath and
789 Simandjuntak, 1983; Spencer et al., 1988). However, this mixture of diamonds with
790 igneous and metamorphic minerals is not surprising considering all of Kalimantan's
791 alluvial diamond deposits are located in close proximity to the Schwaner Granitoids

792 and metamorphic rocks (e.g. Pinoh Metamorphics and Meratus Accretionary
793 Complex) (Figure 1a).
794
795 Subduction-related metamorphic diamonds could represent either the local or distal
796 source of diamonds that we have identified in this study. Diamonds associated with
797 UHP metamorphic rocks are typically very small (<0.1 mm) 'microdiamonds'. Such
798 microdiamonds have been recovered from the Cempaka alluvium and the Meratus
799 Mountains (van Leeuwen, 2014) and are small replicas of the macrodiamonds (e.g.
800 average sizes between 0.1 to 2.0 carats, rare >5 carat, and rarer >20 carat diamonds)
801 (Spencer et al., 1988; van Leeuwen, 2014). The microdiamonds are therefore quite
802 possibly derived from the same source as the macrodiamonds. We therefore suspect
803 that the Cempaka diamonds were not sourced from the UHP metamorphic rocks of
804 the Meratus Accretionaty Complex as there are no reports of macrodiamonds being
805 obtained from exhumed UHP metamorphic rocks, and no UHP mineral phases were
806 recovered from the Cempaka alluvium (e.g. majoritic garnets or abundant rutile
807 inclusions in clinopyroxenes).
808
809 *Insert Figure 17*
810

811 6.1.4 An Asian or Australian Source

812 It is not only Borneo that has alluvial diamonds with an unknown source. Several
813 alluvial diamond deposits are spatially associated with Carboniferous-Permian glacial
814 marine sedimentary units in Myanmar, Thailand and Sumatra (Figure 18) (Griffin et
815 al., 2001; Win et al., 2001). These deposits have been referred to as "Sibumasu
816 Diamonds" due to their distribution within the Sibumasu Terrane (van Leeuwen,

817 2014). They were originally considered as evidence of a connection between India
818 and SE Asia, because diamonds were found in Permian glacial deposits in both
819 Thailand and from Andraha Pradesh in India. This relationship was promoted in some
820 tectonic reconstructions because of fortuitous fitting of coastline morphology and
821 lithologies of similar age (Ridd, 1971). However, we now know that these tectonic
822 reconstructions misposition the major continents and microcontinents relative to what
823 has been determined from seafloor magnetic anomalies and paleomagnetic data (e.g.
824 Hall, 2012; White et al., 2013). We also understand that the Sibumasu and SW
825 Borneo terranes were part of Gondwana (located off the NW Australian margin) until
826 the Early-Middle Permian and Late Jurassic respectively (Metcalfe, 1996; Hall,
827 2012). The discovery of diamonds across Australia in the late 20th century (e.g. Jaques
828 et al., 1986; Atkinson et al., 1990; Jaques 1998), as well as an improved
829 understanding of the tectonic configuration of Gondwana led to speculations that the
830 Sibumasu and Borneo diamonds were possibly derived from crustal fragments of
831 Australian/Gondwanan affinity rather than Indian/Gondwanan affinity (e.g. Taylor et
832 al., 1990; Griffin et al., 2001; Metcalfe, 1996, 2011; Hall, 2012).
833
834 A strong case can be made for the Sibumasu diamonds being derived from an
835 Australian/Gondwanan source as the alluvial diamonds are associated with
836 Carboniferous-Permian diamictites and this combined with paleomagnetic data
837 indicate Sibumasu was part of Gondwana at the time (e.g. Metcalfe, 1996), with the
838 diamonds being deposited before or after Sibumasu was rifted from Gondwana during
839 the Early Permian. By inference a similar origin can be postulated for (some of) the
840 Kalimantan diamonds, which could have been incorporated into the SW Borneo or SE

841 Java blocks before they rifted from NW Australia in the Late Jurassic (Hall, 2012), or
842 were emplaced in these crustal fragments sometime after they rifted (Figure 19).
843
844 Others have proposed that the Sibumasu-Kalimantan diamonds could have been
845 derived from an Australian source based on similarities between particular diamond
846 characteristics. For example, fourier transform infrared (FTIR) spectra from diamonds
847 from Kalimantan, northwestern Australia [Argyle (1.2 Ga: Pidgeon et al., 1989),
848 Ellendale-4 and Ellendale-9 pipes (18-22 Ma: Jaques et al., 1986; Smit et al., 2010;
849 Evans et al., 2013)] and eastern Australia [Copeton] indicates that some of these
850 diamonds share similar mantle residence times and thermal histories (Taylor et al.,
851 1990). This was taken to indicate that the diamonds shared a common origin and may
852 have survived in remnant subcontinental lithospheric mantle beneath Gondwana that
853 was later sampled before or after microcontinents (e.g. SW Borneo) were rifted from
854 Gondwana (Taylor et al., 1990) (this point is discussed further in section 6.2).
855 However, these conclusions are based on relatively common diamond features that
856 are insufficient to show that the Sibumasu-Kalimantan diamonds were obtained from
857 the same source as diamonds in Australia.
858
859 A Gondwanan source of diamonds is plausible in terms of possible sediment transport
860 distances and plate tectonic processes, but such models have been difficult to validate
861 without information on the potential provenance of the material within Borneo's
862 alluvial diamond deposits. The presence of Proterozoic and Archean zircons in the
863 Cempaka deposit and Barito Basin (Figure 9) is a good indication that very old
864 resistant mineral grains such as diamond could have been transported by surficial
865 processes (e.g. alluvial, fluvial transport) or volcanic processes (e.g. xenocrysts

866 brought to the surface during igneous intrusions or eruptions). This is supported by
867 other geochronological studies that have reported inherited Proterozoic and Archean
868 zircons in East Java (due south of Cempaka) (Smyth et al., 2005, 2007) as well as in
869 northwestern and eastern Sulawesi (van Leeuwen et al., 2007; White et al., 2014;
870 Hennig et al., in press). These age data combined with well data and interpretations of
871 offshore seismic data also indicate that Cretaceous or older continental basement
872 extends offshore, north and south of East Java (Emmet et al., 2009; Deighton et al.,
873 2011; Granath et al., 2011).
874
875 Our current understanding of Mesozoic tectonic evolution is that the SE Asian region
876 grew progressively due to the addition of continental fragments over time (e.g.
877 Metcalfe, 1996; Hall, 2012) (e.g. Figure 4). This is particularly well-documented in
878 western Indonesia and more recent work indicates that this is also the case in many
879 parts of eastern Indonesia, such as large parts of west Sulawesi, the Makassar Straits,
880 East Java Sea and East Java (e.g. Metcalfe, 1996; Hall, 2012; Hall and Sevastjanova,
881 2012).
882
883 The growing body of geochronological data (including this study) indicate that the
884 SW Borneo and East Java blocks (Hall, 2012) potentially have Proterozoic to Archean
885 basement and/or sedimentary units that were derived from the erosion of ancient crust
886 (Smyth et al., 2005, 2007; van Leeuwen et al., 2007; White et al., 2014; Hennig et al.,
887 in press). This provides support for the idea that Kalimantan's alluvial diamonds
888 could have been emplaced in thick, ancient crust and/or derived from a distal source,
889 with transport occurring before these terranes were rifted from Gondwana (e.g. Figure
890 19). It also lends support to the idea that these rifted fragments may represent old,

thick crustal fragments in which diamonds may have been emplaced via kimberlites or lamproites that were later reworked and deposited in Kalimantan.

6.2 Multiple diamond sources

We have based our interpretations of the multiple diamond sources primarily on secondary textures (proximal: no wear and tear; distal: a lot of wear and tear). Smith et al. (2009) however, identified five different populations of diamonds across Kalimantan on the basis of primary features in the diamonds, and argued that resorbed, rounded stones were less prone to mechanical abrasion as they were already rounded and hence have the appearance of a proximal stone. Our interpretations differ, but it is agreed that there are diamonds derived from multiple primary igneous sources in Kalimantan (e.g. Smith et al., 2009; van Leeuwen 2014 and references therein). Despite this, one question that remains unanswered is when these diamonds were brought from the sub-continental lithospheric mantle to the shallow crust. A comparative study of several diamonds from the Cempaka deposit with several diamonds from the Australian Ellendale and Copeton deposits addresses this point (Taylor et al., 1990). The Ellendale diamond(s) are associated with lamproites that were brought to the upper crust during the Miocene (18-22 Ma) (Evans et al., 2013). Taylor et al. (1990) compared the results of nitrogen aggregation analyses of Kalimantan, Copeton and Ellendale diamonds. They proposed that diamonds from Kalimantan, Copeton and Ellendale-9 must have been extracted from the mantle at a similar time (150 – 5 Ma) in order for them to plot on the same isotherm. However, subsequent measurements of diamonds from the Copeton and Bingara alluvial deposits indicates that Copeton and Bingara were each derived from distinct sources of different age (Carboniferous and Triassic respectively) (Barron et al., 2011).

916

917 Further characterization of the Kalimantan diamonds is required to determine how
918 long the diamonds resided in the mantle and to identify possible times when they
919 were brought to the surface. Such information could identify feasible mechanisms for
920 diamond emplacement.

921

922 Stratigraphic relations at least provide some information about the relative timing of
923 emplacement as diamonds are found in the basal sequences of Upper Cretaceous to
924 Lower Paleogene sediments (e.g. the Manunggal Formation: Spencer et al., 1988;
925 Guntoro, 1999) in Kalimantan. This requires that some of the Cempaka diamonds
926 must have been emplaced and eroded before the deposition of these units. This
927 implies a local SW Borneo/SE Java source of diamonds during the Cretaceous and/or
928 an older source(s) of diamonds. However, since SW Borneo rifted from Australia in
929 the Late Jurassic (Hall, 2012), diamonds that were brought to the surface after this
930 time (e.g. the model of Taylor et al., 1990) must have been emplaced in a kimberlite
931 or lamproite and could not be alluvial diamonds sourced from the Australian Plate.
932 The lack of diamond indicator minerals around intrusions such as the ~8 Ma Linhaisai
933 Minette (Bergman et al., 1988) indicates they are unlikely to be the source of
934 diamonds but similar undiscovered young potassic or ultrapotassic alkaline volcanics
935 and dykes (Simanjuntak and Simanjuntak, 2000) are a potential local source.

936

937 We favour models where Kalimantan's alluvial diamonds were derived from a local
938 source and were also possibly transported from Gondwana on fragments that were
939 rifted from Gondwana during the Late Jurassic (e.g. SW Borneo / SE Java blocks)
940 (Metcalfe, 1996, 2011; Hall, 2012; Hall and Sevastjanova, 2012) (Figure 19). The

941 diamonds were unlikely to have been sourced from the Sibumasu Terrane by transport
942 along major Asian fluvial systems because parts of Sundaland (e.g. the Tin Belt and
943 western Borneo) have been elevated at least since the Late Cretaceous (Figure 18). It
944 is more likely that the material in the Cempaka alluvium was derived from the erosion
945 of nearby rocks in the Schwaner and Meratus mountains and in the Barito Basin,
946 along with material being transported from paleo-highs such as the Karimunjawa
947 Arch to the south which provided material that was originally the sedimentary cover
948 to the SW Borneo and East Java blocks (e.g. Witts et al., 2011). Future studies should
949 test these ideas further, and one way to do this would be to characterise the age and
950 morphology of diamonds, zircons and other heavy minerals from the Manunggal
951 Formation to determine if the 'younger', less reworked diamonds that are present at
952 Cempaka are also found in these older sediments.
953
954
955 **7. Conclusion**
956 Geochronological and geochemical data provide new evidence on possible sources of
957 clastic material that accumulated in Kalimantan's Cempaka alluvial diamond deposit.
958 Our results show that the Cempaka diamonds can be divided into two groups, one (A)
959 that was transported from a distal source and/or were recycled several times
960 indicating a long history in the secondary environment, the other (B) was not. The
961 presence of diamonds in Upper Cretaceous paleo-alluvials indicates that at least some
962 of the diamonds were already present in Borneo in the Early Cretaceous or earlier.
963 Group A diamonds are obvious candidates and were most likely emplaced in the SW
964 Borneo fragment and reworked several times, or were transported from NW Australia
965 to the SW Borneo fragment before it rifted from Gondwana in the Late Jurassic.

966 Group B diamonds are unlikely to have been sourced from the erosion of nearby
967 ophiolites or ultra-high pressure metamorphic rocks exposed in the nearby Meratus
968 Mountains, because of the high proportion of macrodiamonds and because no mineral
969 phases indicative of UHP metamorphism have been found within the Cempaka
970 alluvium. However, the widespread occurrence of Miocene alkaline igneous bodies in
971 the central part of Borneo indicates that the Neogene tectonic environment was
972 conducive for the emplacement of diamondiferous diatremes or mantle-penetrating
973 faults that could tap diamond-bearing material. These could explain the Group B
974 diamonds that show little evidence of reworking.
975
976 **Acknowledgements**
977 L.T.W, D.T. and R.H. wish to thank the Southeast Asia Research Group consortium
978 members for partially funding this work. We thank Sue Lindsay and Gayle Webb
979 from the Australian Museum for assisting with zircon SEM imagery and diamond
980 photography as well as Doug Austen for polishing the windows on the ballas and
981 diamond grains. Steve Bergman, Ian Metcalf and an anonymous reviewer are thanked
982 for reviewing this manuscript. We would also like to thank Lynton Jaques for
983 providing feedback on an earlier draft.
984
985 **References**
986 Atkinson, W.A., Smith, C.B., Danchin, R.V., Janse, B.A., 1990. Diamonds in
987 Australia. In Hughes, F.E. (ed.), Geology of mineral deposits of Australia and
988 Papua New Guinea. Australasian Institute of Mining and Metallurgy, Melbourne,
989 69-76.

990 Barnes, S.J., Roeder, P.L., 2001. The range of spinel compositions in terrestrial mafic
991 and ultramafic rocks. Journal of Petrology 42, 2279-2302.
992 Barron, L., Mernagh, T.P., Pogson, R., Barron, B.J., 2008a. Alluvial Ultrahigh
993 Pressure (UHP) macrodiamond at Copeton/Bingara (Eastern Australia), and
994 Cempaka (Kalimantan, Indonesia). 9th International Kimberlite Conference
995 Extended Abstract No. 9IKC-A-00039 1–3.
996 Barron, L. M., Barron, B. J., Mernagh, T. P., Birch, W. D., 2008b. Ultrahigh pressure
997 macrodiamonds from Copeton (New South Wales, Australia), based on Raman
998 spectroscopy of inclusions. Ore Geology Reviews 34, 76-86.
999 Barron, L., Mernagh, T. P., Barron, B. J., Pogson, R., 2011. Spectroscopic research on
1000 ultrahigh pressure (UHP) macrodiamond at Copeton and Bingara NSW, Eastern
1001 Australia. Spectrochimica Acta Part A: Molecular and Biomolecular
1002 Spectroscopy 80, 112-118.
1003 Belousova, E., Griffin, W., O'reilly, S.Y., Fisher, N., 2002. Igneous zircon: trace
1004 element composition as an indicator of source rock type. Contrib Mineral Petrol
1005 143, 602–622. doi:10.1007/s00410-002-0364-7
1006 Bergman, S.C., Dunn, D.P., Krol, L.G., 1988. Rock and mineral chemistry of the
1007 Linhaisai minette, central Kalimantan, Indonesia, and the origin of Borneo
1008 diamonds. Canadian Mineralogist 26, 23–43.
1009 Bergman, S.C., Turner, W.S., Krol, L.G., 1987. A reassessment of the diamondiferous
1010 Pamali Breccia, southeast Kalimantan, Indonesia: Intrusive kimberlite breccia or
1011 sedimentary conglomerate? Geological Society of America Special Papers 215,
1012 183–196.
1013 Bergman, S.C., Coffield, D.Q., Talbot, J.P., Garrard, A., 1996. Tertiary Tectonic and
1014 magmatic evolution of western Sulawesi and the Makassar Strait, Indonesia:

1015 evidence for a Miocene continent-continent collision, in: Hall, R. and Blundell,
1016 D., (Eds.), Tectonic Evolution of Southeast Asia, Geological Society Special
1017 Publications 106, 391-429.
1018 Bernet, M., Garver, J. I., 2005. Fission-track Analysis of Detrital Zircon. Reviews in
1019 Mineralogy & Geochemistry 58, 205-238.
1020 Black, L., Kamo, S., Allen, C., Davis, D., Aleinikoff, J., Valley, J., Mundil, R.,
1021 Campbell, I., Korsch, R., Williams, I.S., 2004. Improved 206Pb/238U
1022 microprobe geochronology by the monitoring of a trace-element-related matrix
1023 effect; SHRIMP, ID–TIMS, ELA–ICP–MS and oxygen isotope documentation
1024 for a series of zircon standards. Chemical Geology 205, 115–140.
1025 Bosshart, G., 1998. Diamonds of natural green body colour. Proceedings of the
1026 Brazilian Geological Congress. Belo Horizonte, Brazil.
1027 Burgath, K. P., Simandjuntak, H. R. W., 1983. Investigation of ophiolite suites and
1028 their mineral possibilities in Southeast Kalimantan. Unpublished Report Federal
1029 Institute for Geosciences and Natural Resources and Directorate of Mineral
1030 Resources, pp. 26.
1031 Burgath, K.P., Mohr, M., 1991. The Pamali Breccia near Martapura in South-East
1032 Kalimantan (Indonesia Borneo) - a diamondiferous diatreme? Geologische
1033 Jahrbuch A 127, 569–587.
1034 Carter, A., Bristow, C.S. 2003. Linking hinterland evolution and continental basin
1035 sedimentation by using detrital zircon thermochronology: a study of the Khorat
1036 Plateau Basin, eastern Thailand. Basin Research 15, 271-285.
1037 Carter, A., Moss, S.J. 1999. Combined detrital-zircon fission-track and U-Pb dating:
1038 A new approach to understand hinterland evolution. Geology 27, 235-238.

1039 Claoué-Long, J. C., Compston, W., Roberts, J. and Fanning, C. M., 1995. Two
1040 Carboniferous ages: a comparison of SHRIMP zircon dating with conventional
1041 zircons ages and $^{40}Ar/^{39}Ar$ analysis. In: Geochronology, Time Scales and Global
1042 Stratigraphic Correlation, Berggen, W. A., Kent, D. V., Aubry, M. P. and
1043 Hardenbol, J. (eds.), Vol. 4, pp. 3-21. SEPM Special Publication.
1044 Clements, B., Burgess, P., Hall, R., Cottam, M. A. 2011. Subsidence and uplift by
1045 slab-related mantle dynamics: a driving mechanism for the Late Cretaceous and
1046 Cenozoic evolution of continental SE Asia? In Hall, R., Cottam, M. A. and
1047 Wilson, M. E. J. (Eds.). The SE Asian Gateway: History and Tectonics of the
1048 Australia-Asia Collision. Geological Society of London, Special Publications
1049 355, 37-51.
1050 Davies, A. G. S., Cooke, D. R., Gemmell, J. B. 2008. Hydrothermal Breccias and
1051 Veins at the Kelian Gold Mine, Kalimantan, Indonesia: Genesis of a Large
1052 Epithermal Gold Deposit. Economic Geology 103, 717-757.
1053 Davies, L., Hall, R., Armstrong, R.A., 2014. Cretaceous crust in SW Borneo:
1054 Petrological, geochemical and geochronological constraints from the Schwaner
1055 Mountains. Proceedings Indonesian Petroleum Association, 38th Annual
1056 Convention, IPA14-G-025 1-15.
1057 Deighton, I., Hancock, T., Hudson, G., Tamannai, M., Conn, P., Oh, K., 2011. Infill
1058 seismic in the southeast Java forearc basin: implications for petroleum
1059 prospectivity. Proceedings Indonesian Petroleum Association, 35th Annual
1060 Convention, IPA11-G-068, 1-14.
1061 Eggins, S. M., 2003. Laser ablation analysis of geological materials as lithium borate
1062 glasses. Geostandards Newsletter 27, 147-162

1063 Eggins, S. M., Kinsley, L. K., Shelley, J. M. G., 1998. Deposition and element
1064 fractionation processes occurring during atmospheric pressure laser sampling for
1065 analysis by ICPMS. Applied Surface Science 127-129, 278-286.
1066 Eggins, S. M., Rudnick, R. L., McDonough, W. F., 1998. The composition of
1067 peridotites and their minerals: a laser-ablation study. Earth and Planetary Science
1068 Letters 154, 53-71.
1069 Emmet, P.A., Granath, J.W., Dinkelman, M.G., 2009. Pre-Tertiary sedimentary
1070 "keels" provide insights into tectonic assembly of basement terranes and present-
1071 day petroleum systems of the East Java Sea. Proceedings Indonesian Petroleum
1072 Association 33rd Annual Convention, Jakarta, IPA09-G-046, 1-11.
1073 Evans, N.J., McInnes, B.I.A., McDonald, B., Danišík, M., Jourdan, F., Mayers, C.,
1074 Thern, E., Corbett, D., 2013. Emplacement age and thermal footprint of the
1075 diamondiferous Ellendale E9 lamproite pipe, Western Australia. Mineralium
1076 Deposita 48, 413–421. doi:10.1007/s00126-012-0430-7
1077 Fipke, C.E., Gurney, J.J., Moore, R.O., Nassichuck, W.W., 1989. The development of
1078 advanced technology to distinguish between diamondiferous and barren
1079 diatremes. Geological Survey of Canada Open File Report 2124, 621 pp.
1080 Galbraith, R.F., 1988. Graphical display of estimates having different standard errors.
1081 Technometrics, 30, 271-281.
1082 Galbraith, R.F., 1990. The radial plot: graphical assessment of spread in ages. Nuclear
1083 tracks, 5, 207-214.
1084 Gleadow, A.J.W., Hurford, A.J., and Quaife, R.D., 1976. Fission track dating of
1085 zircon: improved etching techniques. Earth and Planetary Science Letters, 33:
1086 273-276.

1087 Gordeev, E.I., Karpov, G.A., Anikin, L.P., Krivovichev, S.V., Filatov, S.K., Antonov,
1088 A.V., Ovsyannikov, A.A. 2014. Diamonds in Lavas of the Tolbachik Fissure
1089 Eruption in Kamchatka. Doklady Earth Sciences 454, 47-49.
1090 Govindaraju, K., Potts, P. J., Webb, P. C., Watson, J. S. 1994. 1994 Report on Whin
1091 Sill dolerite WS-E from England and Pitscurrie Microgabbro PM-S from
1092 Scotland: Assessment by one hundred and four international laboratories.
1093 Geostandards Newsletter, 18, 211-300.
1094 Graham, I., Grieve, T., Spencer, L., Hager, S., 2014. Source of PGM and gold from
1095 the Cempaka palaeoplacer deposit, SE Kalimantan, Indonesia..12th International
1096 Platinum Symposium (abstracts), Edited by Anikina, E. V. et al., Yekaterinburg:
1097 Institute of Geology and Geochemistry. ISBN 978-5-94332-109-2, pp. 173.
1098 Granath, J.W., Christ, J.M., Emmet, P.A., Dinkelman, M.G., 2011. Pre-Cenozoic
1099 sedimentary section and structure as reflected in the JavaSPAN crustal-scale
1100 PSDM seismic survey, and its implications regarding the basement terranes in the
1101 East Java Sea. In: Hall, R., Cottam, M. A. & Wilson, M. E. J. (Eds.), The SE
1102 Asian Gateway: History and Tectonics of the Australia-Asia collision. Geological
1103 Society of London Special Publication 355, 53–74. doi:10.1144/SP355.4
1104 Green, P. F. 1981. A new look at statistics in fission track dating. Nuclear Tracks, 5,
1105 77-86.
1106 Green, P.F., 1985. A comparison of zeta calibration baselines in zircon, sphene and
1107 apatite. Chemical Geology, 58: 1-22.
1108
1109 Griffin, W.L., Win, T.T., Davies, R., Wathanakul, P., Andrew, A., Metcalfe, I.,
1110 Cartigny, P., 2001. Diamonds from Myanmar and Thailand: Characteristics and
1111 Possible Origins. Economic Geology 96, 159–170.

1112 Guntoro, A., 1999. The formation of the Makassar Strait and the separation between
1113 SE Kalimantan and SW Sulawesi. Journal of Asian Earth Sciences 17, 79-98.
1114 Hall, R., 2012. Late Jurassic–Cenozoic reconstructions of the Indonesian region and
1115 the Indian Ocean. Tectonophysics 570-571, 1–41.doi:10.1016/j.tecto.2012.04.021
1116 Hall, R., 2013. The paleogeography of Sundaland and Wallacea since the Late
1117 Jurassic. Journal of Limnology 72, 1-17.
1118 Hall, R., 2014. The origin of Sundaland. Proceedings of Sundaland Resources MGEI
1119 Annual Convention, Palembang, South Sumatra, Indonesia, 25 pp.
1120 Hall, R., Sevastjanova, I., 2012. Australian crust in Indonesia. Australian Journal of
1121 Earth Sciences 59, 827-844.
1122 Hamilton, W., 1979. Tectonics of the Indonesian region. USGS Professional Paper
1123 1078, 345 pp.
1124 Hartano, U., Dirk, M. H. J., Sanyoto, P., Permanadewi, S., 1999. Geochemistry and
1125 K/Ar results of the Mesozoic-Cenozoic plutonic and volcanic rocks from the
1126 Meratus Range, South Kalimantan. GEOSEA ’98 Proceedings, Geological
1127 Society of Malaysia Bulletin, 43. 49-61.
1128 Hattori, K., Burgath, K. -P., Hart, S. R., 1992. Os-isotope study of platinum-group
1129 minerals in chromitites in Alpine-type ultramafic intrusions and the associated
1130 placers in Borneo. Mineralogical Magazine, 56, 157-164.
1131 Hattori, K. H., Cabri, L. J. Johanson, B., Zientek, M. L. 2004. Origin of placer laurite
1132 from Borneo: Se and As contents, and S isotopic compositions. Mineralogical
1133 Magazine, 68, 353-368.
1134 Hennig, J., Hall, R., Armstrong, R.A., (In press). U-Pb zircon geochronology of rocks
1135 from west Central Sulawesi, Indonesia: Extension-related metamorphism and

1136 magmatism during the early stages of mountain building. Gondwana Research.
1137 doi:10.1016/j.gr.2014.12.012
1138 Jaques, A.L., 1998. Kimberlite and lamproite diamond pipes. AGSO Journal of
1139 Australian Geology and Geophysics 17, 153–162.
1140 Jaques, A.L., 2005. Australian diamond deposits, kimberlites, and related rocks
1141 1:5,000,000 scale map. Geoscience Australia, Canberra .
1142 Jaques, A.L., Lewis J.D., Smith C.B., 1986. The kimberlites and lamproites of
1143 Western Australia. Geological Survey of Western Australia Bulletin 132, 267pp.
1144 Karpov, G.A., Silaev, V.I., Anikin, L.P., Rakin, V.I., Vasil'ev, E.A., Filatov, S.K.,
1145 Petrovskii, V.A., and Flerov, G.B., 2014. Diamonds and Accessory Minerals in
1146 Products of the 2012-2013 Tolbachik Fissure Eruption. Journal of Volcanology
1147 and Seismology 8, 323-339.
1148 Katili, J. A. 1978. Past and present geotectonic position of Sulawesi, Indonesia.
1149 Tectonophysics 45, 289-322.
1150 Kolff, L., 2010. Timber Creek ERL 25981 – Final diamond recovery and mineral
1151 chemical data. Mineral exploration report for the Northern Territory Geological
1152 Survey.
1153 Koolhoven, W. C. B., 1935. The primary occurrence of South Borneo diamonds:
1154 Geologisch-Mijbouwkundig Genootschap voor Nederland en Kolonien,
1155 verhandelingen, Geologische serie 9, 189-232.
1156 Krol, L. H., 1919. The diamonds of Borneo, their deposits and workings. Amsterdam,
1157 De Mijningenieur, p. 707-709.
1158 Krol, L. H., 1922. Bijdrage tot de kennis van de oorsprong en de verspreiding der
1159 diamanthoudende afzettingen in ZO. Borneo. Jaarboek van het Mijnwezen 49,
1160 250-304.

1161 Lennie, D. 1997. Diamond and gold potential Central Kalimantan; unpublished report
1162 prepared for South Pacific Resources, pp 50.
1163 Lister, G., Forster, M.A., 2009. Tectonic mode switches and the nature of orogenesis.
1164 Lithos 113, 274–291.
1165 Longerich, H. P., Jackson, S. E., Gunther, D. 1996. Inter-laboratory note. Laser
1166 ablation inductively coupled plasma mass spectrometric transient signal data
1167 acquisition and analyte concentration calculation. Journal of Analytical Atomic
1168 Spectrometry 11, 899-904.
1169 Ludwig, K., 2009. SQUID 2, A User's Manual, rev. 12 April 2009; Berkeley
1170 Geochronological Centre Special Publication 5, 110 pp.
1171 Ludwig, K. R., 2003. Isoplot 3.00: A Geochronological Toolkit for Microsoft Excel.
1172 Berkeley Geochronological Centre Special Publication No. 4, 70 pp.
1173 Metcalfe, I., 1996. Pre-Cretaceous evolution of SE Asian Terranes. In: Hall, R. &
1174 Blundell, D. J. (Eds.), Tectonic Evolution of SE Asia. Geological Society of
1175 London Special Publication, 106, 97-122.
1176 Metcalfe, I. 2011. Tectonic framework and Phanerozoic evolution of Sundaland.
1177 Gondwana Research 19, 3-21.
1178 Metcalfe, I., 2013. Gondwana dispersion and Asian accretion: Tectonic and
1179 palaeogeographic evolution of eastern Tethys. Journal of Asian Earth Sciences
1180 66, 1-33.
1181 Mitchell, R.H., Bergman S.C. 1991. Petrology of Lamproites. Springer, New York.
1182 447 pp. doi: 10.1007/978-1-4615-3788-5
1183 Miyashiro, A. 1994. Metamorphic Petrology. UCL Press Limited, London, 404p.
1184 Muller, J. 1968. Palynology of the Pedawan and Plateau Sandstone Formations
1185 (Cretaceous-Eocene) in Sarawak, Malaysia. Micropaleontology 14, 1-37.

1186 Nixon, P.H., Bergman, S.C., 1987. Anomalous Occurrences of Diamonds. Indiaqua
1187 47, 21–27.
1188 Parkinson, C.D., Miyazaki, K., Wakita, K., Barber, A.J., Carswell, D.A., 1998. An
1189 overview and tectonic synthesis of the pre-Tertiary very-high-pressure
1190 metamorphic and associated rocks of Java, Sulawesi and Kalimantan, Indonesia.
1191 The Island Arc 7, 184–200.
1192 Pidgeon, R.P., Smith, C.B., Fanning, C.M. 1989. Emplacement ages of kimberlites
1193 and lamproites in Western Australia. In Kimberlites and Related Rocks: I. Their
1194 Composition, Occurrence, Origin and Emplacement. Proceedings of the Fourth
1195 International Kimberlite Conference, Perth, 1986, vol. 14 (ed. J. Ross).
1196 Geological Society of Australia Special Publication, Blackwell Scientific
1197 Publications, pp. 369–381.
1198 Pownall, J.M., Hall, R., Armstrong, R.A., Forster, M.A., 2014. Earth's youngest
1199 known ultrahigh-temperature granulites discovered on Seram, eastern Indonesia.
1200 Geology 42, 279–282. doi:10.1130/G35230.1
1201 Pownall, J.M., Hall, R., Watkinson, I.M., 2013. Extreme extension across Seram and
1202 Ambon, eastern Indonesia: evidence for Banda slab rollback. Solid Earth 4, 277–
1203 314. doi:10.5194/se-4-277-2013
1204 Ridd, M.F., 1971. South-East Asia as a part of Gondwanaland. Nature 234, 531–533.
1205 Robinson, P. T., Trumbull, R., Yang, J. S., Schmitt, A. 2011., Deep subduction of
1206 crustal minerals in the mantle: Evidence from ophiolites. Goldschmidt 2011
1207 Conference Abstracts, Mineralogical Magazine 77, 1736.
1208 Rocholl, A., 1998. Major and Trace Element Composition and Homogeneity of
1209 Microbeam Reference Material: Basalt Glass USGS BCR-2G. Geostandards
1210 Newsletter 22, 33-45.

1211 Sambridge, M. S., Compston, W., 1994. Mixture modeling of multicomponent data
1212 sets with application to ion-probe zircon ages. Earth and Planetary Science
1213 Letters 128, 373-390.
1214 Scheibner, E., Basden, H. (Editors), 1998. Geology of New South Wales. Synthesis.
1215 Volume 2 Geological Evolution. Geological Survey of New South Wales Memoir
1216 Geology 13(2).
1217 Seavoy, R.E., 1975. Placer Diamond Mining in Kalimantan, Indonesia. Indonesia 19,
1218 79–84, doi:10.2307/3350703
1219 Shirey, S. B., Cartigny, P., Frost, D. J., Keshav, S., Nestola, F., Nimis, P., Pearson, D.
1220 G., Sobolev, N. V., Walter, M. J., 2013. Diamonds and the Geology of Mantle
1221 Carbon. Reviews in Mineralogy & Geochemistry 75, 355-421.
1222 Sigit, S., Purbo-Hadiwidjojo, M. M., Sulasumoro, B., and Wirjosudjon, S., 1969.
1223 Minerals and mining in Indonesia: Jakarta, Ministry of Mines, 123 pp.
1224 Sikumbang, N., 1990. The geology and tectonics of the Meratus Mountains, South
1225 Kalimantan, Indonesia. Geologi Indonesia, Journal of the Indonesian Association
1226 of Geologists 13, 1-31.
1227 Simandjuntak, H. R. W., Simandjuntak, T. O., 2000. Kalimantan diamond; The
1228 prospect and potential of placer diamond and the possibility of primary diamond
1229 occurrences. Directorate of Mineral Resources, Special Publication of the DMR,
1230 pp. 44.
1231 Smit, K.V., Shirey, S.B., Richardson, S.H., le Roex, A.P., Gurney, J.J., 2010. Re–Os
1232 isotopic composition of peridotitic sulphide inclusions in diamonds from
1233 Ellendale, Australia: Age constraints on Kimberley cratonic lithosphere. Name:
1234 Geochim. Cosmochim. Acta 74, 3292–3306. doi:10.1016/j.gca.2010.03.001

1235 Smith, C.B., Bulanova, G.P., Kohn, S.C., Milledge, H.J., Hall, A.E., Griffin, B.J.,
1236 Pearson, D.G., 2009. Nature and genesis of Kalimantan diamonds. Lithos 112,
1237 822–832. doi:10.1016/j.lithos.2009.05.014
1238 Smyth, H.R., Hall, R., Hamilton, J., Kinny, P., 2005. East Java: Cenozoic basins,
1239 volcanoes and ancient basement. Indonesian Petroleum Association, Proceedings
1240 30th Annual Convention, 251-266.
1241 Smyth, H.R., Hamilton, P.J., Hall, R., Kinny, P.D., 2007. The deep crust beneath
1242 island arcs: Inherited zircons reveal a Gondwana continental fragment beneath
1243 East Java, Indonesia. Earth and Planetary Science Letters 258, 269–282.
1244 doi:10.1016/j.epsl.2007.03.044
1245 Soeria-Atmajda, R., Noeradi, D., Priadi, B., 1999. Cenozoic magmatism in
1246 Kalimantan and its related geodynamic evolution. Journal of Asian Earth
1247 Sciences 17, 25-45.
1248 Spencer, L. K., Watson, C. 2002. Feasibility study of Cempaka Diamond Mine. P.T.
1249 Galuh Cempaka (unpublished).
1250 Spencer, L.K., Dikinis, S.D., Keller, P. C., Kane, R.E., 1988. The diamond deposits of
1251 Kalimantan, Borneo. Gems and Gemology 67–80.
1252 Steiger, R. H., and Jäger, E. 1977. Subcomission on geochronology: convention on
1253 the use of decay constants in geo- and cosmochronology. Earth and Planetary
1254 Science Letters, 36, 359-362.
1255 Sumartadipura, S. 1976. Geologic map of the Tewah quadrangle, Kalimantan.
1256 (1:250,000). Explanatory note and geological map. Geological Survey of
1257 Indonesia, Ministry of Mines, Bandung, Indonesia, 1-5.

1258 Sun, T. T., Wathanakul, P., Atichat, W., Moh, L. H., Kem, L.K., and Hermanto, R.,
1259 2005. Kalimantan Diamond: Morphology, surface features and some
1260 spectroscopic approaches. Australian Gemmologist 22, 186-195.
1261 Swamidharma, Y. C. A., Khoirruzukin, A., Cahyadi, Krunanto, Y., Herkosuma, D.,
1262 2015. Mineral resource and potential in ultramafic cumulate complex of Sebuku
1263 Island. Proceedings MGEI 7th Annual Convention "Indonesia's mineral and coal
1264 resources: Discovery to inventory, p. 131-136.
1265 Taylor, W.R., Jaques, A.L., Ridd, M., 1990. Nitrogen-defect aggregation
1266 characteristics of some Australasian diamonds: Time-temperature constraints on
1267 the source regions of pipe and alluvial diamonds. American Mineralogist 75,
1268 1290–1310.
1269 van Bemmelen, R. W., 1949. The Geology of Indonesia, Volume II Economic
1270 Geology. Government Printing Office, The Hague, pp. 265.
1271 van Leeuwen, T. M., Leach, T., Hawke, A. A. and Hawke, M. M. 1990. The Kelian
1272 disseminated gold deposit, East Kalimantan, Indonesia. Journal of Geochemical
1273 Exploration 35, 1-61.
1274 van Leeuwen, T. M., 1994. 25 Years of mineral exploration and discovery in
1275 Indonesia. Journal of Geochemical Exploration 50, 13-90.
1276 van Leeuwen, T., 2014. The enigmatic Sundaland Diamonds - a review In:
1277 Proceedings of Sundaland Resources 2014 MGEI Annual Convention 17-18
1278 November 2014, pp. 181-204, Palembang, Sumatra, Indonesia.
1279 van Leeuwen, T., Allen, C.M., Kadarusman, A., Elburg, M., Palin, J. M., Muhardjo,
1280 Suwijanto, 2007. Petrologic, isotopic, and radiometric age constraints on the
1281 origin and tectonic history of the Malino Metamorphic Complex, NW Sulawesi,

1282 Indonesia. Journal of Asian Earth Sciences 29, 751–777.
1283 doi:10.1016/j.jseaes.2006.05.002
1284 Vance, E. R., Harris, J. W., Milledge, H.J. 1973. Possible origins of α-damage in
1285 diamonds from kimberlite and alluvial sources. Mineralogical Magazine 39
1286 (303), 349-360.
1287 Wagner, C., 1986. Mineralogy of the type kajanite from Kalimantan. Similarities and
1288 differences with typical lamproites. Bulletin Minéralogie 109, 589-598.
1289 Wakita, K., Miyazaki, K., Zulkarnein, L., Sopaheluwakan, J., Sanyoto, 1998.
1290 Tectonic implications of new age data for the Meratus complex of south
1291 Kalimantan, Indonesia. Island Arc 7, 202-222.
1292 White, L.T., Gibson, G.M., Lister, G.S., 2013. A reassessment of paleogeographic
1293 reconstructions of eastern Gondwana: Bringing geology back into the equation.
1294 Gondwana Research 24, 984–998. doi:10.1016/j.gr.2013.06.009
1295 White, L.T., Hall, R., Armstrong, R.A., 2014. The age of undeformed dacite
1296 intrusions within the Kolaka Fault zone, SE Sulawesi, Indonesia. Journal of
1297 Asian Earth Sciences 94, 105–112. doi:10.1016/j.jseaes.2014.08.014
1298 Wiedenbeck, M., Allé, P., Corfu, F., Griffin, W. L., Meier, M., Oberli, F., Von Quadt,
1299 A., Roddick, J. C., Spiegel, W. 1995. Three natural zircon standards for U-Th-Pb,
1300 Lu-Hf, trace element and REE analyses. Geostandards Newsletter, 19, 1-23.
1301 Williams, I. S. 1998. U-Th-Pb geochronology by ion microprobe. In: Reviews of
1302 microanalytical techniques to understanding mineralizing processes, McKibben,
1303 M. A., Shanks, III, W. C. and Ridley, W. I. (eds.), Reviews in Economic
1304 Geology, 7, 1-35.

1305 Win, T.T., Davies, R.M., Griffin, W.L., Wathanakul, P., French, D.H., 2001.
1306 Distribution and characteristics of diamonds from Myanmar. Journal of Asian
1307 Earth Sciences 19, 563–577.
1308 Witts, D., Hall, R., Morley, R.J., BouDagher-Fadel, M.K., 2011. Stratigraphy and
1309 sediment provenance, Barito Basin, Southeast Kalimantan. Proceedings
1310 Indonesian Petroleum Association, 35th Annual Convention, IPA11-G-054.
1311 Witts, D., Hall, R., Nichols, G., Morley, R., 2012.A new depositional and provenance
1312 model for the Tanjung Formation, Barito Basin, SE Kalimantan, Indonesia.
1313 Journal of Asian Earth Sciences 56, 77–104. doi:10.1016/j.jseaes.2012.04.022
1314 Yang, J-. S., Robinson, P. T., Dilek, Y. 2014. Diamonds in Ophiolites. Elements 10,
1315 127-130 (doi: 10.2113/gselements.10.2.127).
1316 Zientek, M.L., Pardiarto, B., Simandjuntak, H.R.W., Wikrama, A., Oscarson, R.L.,
1317 Meier, A.L., Carlson, R.R., 1992. Placer and lode platinum group minerals in
1318 South Kalimantan, Indonesia: Evidence for derivation from Alaskan-type
1319 ultramafic intrusions. Australian Journal of Earth Sciences 39, 405–417.
1320 doi:10.1080/08120099208728033
1321
1322
1323

Figure Captions

Figure 1. (a) Map of Borneo showing the location of Cempaka and other alluvial diamond deposits across Kalimantan (modified from Smith et al., 2009), as well as the location of geological units discussed in this study. (b) An example of one of the conglomeratic units in which the Cempaka alluvial diamonds are found.

Figure 2. Schematic diagram showing the tectonic setting of diamond formation. Diamonds are stable at depths of approximately 150 km and are typically sourced from sub-continental lithospheric mantle beneath thick continental crust (a 'craton'), where they are brought to the surface as xenocrysts in kimberlite and lamproite intrusions. They may also be generated at similar depths in subducted oceanic crust and potentially brought to the surface with UHP metamorphic rocks (modified after Shirey et al., 2013).

Figure 3. Two tectonic reconstructions of SE Asia during the Lower Cretaceous [(a) 130 Ma and (b) 120 Ma] to show Borneo's position at the time with respect to Australia, Sundaland and other parts of what is now SE Asia. SWB = South West Borneo Block, EJWS = East Java/West Sulawesi Block; Sc.P. = Scott Plateau; Ex. P. = Exmouth Plateau; East C-T = East Ceno Tethys. Images taken from Hall (2012).

Figure 4. Regional map showing the location of Sundaland and the various crustal blocks that define it as well as when each of the fragments were rifted from Gondwana and when these accreted to the Asian margin (modified from Metcalfe, 1996, 2011; Hall and Sevastjanova, 2012).

1349 Figure 5. Provenance of Cempaka spinels (grey diamonds) compared with the 50th
1350 and 30th percentiles of a global spinel composition database (Barnes and Roeder,
1351 2001) for ophiolites excluding chromite seams (blue), kimberlite (yellow) and
1352 lamproites (red). These data show that the Cempaka spinels are dominantly sourced
1353 from an ophiolite, rather than a kimberlite or lamproite. Note, for simplicity only
1354 three geological environments are shown here. Readers are directed to the global
1355 spinel database (Barnes and Roeder, 2001) for more details about the compositional
1356 ranges of other settings.
1357
1358 Figure 6. Conventional U-Pb concordia plots of the results obtained from SHRIMP U-
1359 Pb isotopic analyses of Cempaka detrital zircons, showing (a) the full range of age
1360 data obtained, and (b) the majority of age data, which are less than 600 Ma.
1361
1362 Figure 7. CL imagery of Cempaka detrital zircons as well as the location and result of
1363 each SHRIMP analysis, marked with yellow and red circles. This data shows that the
1364 majority of zircons are primarily oscillatory zoned igneous zircons, some also
1365 showing sector zoning and generally lack overgrowths (i.e. rims). The zircons that are
1366 younger than ~120 Ma are predominantly angular, euhedral grains or angular grain
1367 fragments (shown with yellow circles), whereas older grains are generally rounded to
1368 angular, indicating that many such grains have been reworked.
1369
1370

1371 Figure 8. Secondary electron SEM images of non-polished zircon grains, including:
1372 (a-c) rounded and sub-rounded grains which are indicative of transport in a high
1373 energy environment for some time; and (d-i) euhedral angular grains, many of which
1374 preserve primary growth textures [e.g. (e) and (f)], preserved mineral inclusions [e.g.
1375 (d)] or zones where mineral inclusions have been chemically or mechanically
1376 removed [e.g. (g) and (i). These features would not be preserved with prolonged
1377 transport in a high energy environment.
1378
1379 Figure 9. Relative frequency plots of zircon ages obtained from (a-b) Cempaka (this
1380 study) compared with zircon ages obtained from the (c-d) Schwaner Granitoids
1381 (modified from Davies et al., 2014); (e-f) Pinoh Metamorphics (modified from Davies
1382 et al. 2014); (g-h) Barito Basin (Witts et al., 2011, 2012), and (i-j) the Khorat Plateau
1383 Basin (Carter and Moss, 1999; Carter and Bristow, 2003).
1384
1385 Figure 10. Relative probability-frequency plot of age zircon fission-track age data
1386 obtained from twenty detrital zircons from the Cempaka alluvial deposit. The plot
1387 shows the results of zircon fission track analyses of two size fractions of zircons (<1
1388 mm and >1mm).
1389
1390 Figure 11. Comparison of the mode (white dot) and range (red line) of trace element
1391 results obtained from LA-ICPMS analyses of zircon from (a) Cempaka, compared
1392 with average compositions of zircons reported from (b) lamproites*; (c) kimberlites*;
1393 (d) basalts*; and (e) granitoids* [*Data from Belousova et al., (2002)]. The trace
1394 element data also indicates that different compositional groups can be identified,
1395 particularly when the trace element data is plotted according to different grain-size

1396 populations and when age data can be incorporated into the interpretation [e.g. (f) Hf
1397 vs. Ce plot].
1398
1399 Figure 12. Photomicrographs of Cempaka diamond morphologies: (a) modified
1400 colourless tetrahexahedron with fine plastic deformation lamellae (4 mm), (b)
1401 relatively flattened colourless octahedron (i.e. macle) with graphite inclusions (3
1402 mm), (c) twinned cubo-octahedron with pronounced brown radiation spots (4 mm),
1403 and (d) partially resorbed dodecahedron (2 mm).
1404
1405 Figure 13. Photomicrographs of Cempaka semi-opaque to opaque diamonds: (a) semi-
1406 opaque cubo-octohedral diamond with polished window (2 mm); (b) close-up view of
1407 (a) through the polished window showing distinctive platy black graphite aligned
1408 along crystallographic planes (FOV ~0.1 mm); (c) modified cubo-octahedra opaque
1409 diamond (2 mm), and (d) anhedral semi-ovoid rough-textured ballas (3 mm).
1410
1411 Figure 14. Photomicrographs of (a) Cempaka diamonds with radiation “spots”, and
1412 (b-d) cut “windows” showing the internal structure of Cempaka diamonds. (a) The
1413 green outer colour is due to the presence of green-coloured radiation “spots” (this
1414 diamond has a length of 2 mm). (b) Cut window through semi-opaque coated
1415 diamond showing its transparent interior (FOV is ~0.2 mm); (c) Cut window through
1416 semi-opaque coated diamond showing abundant near-surface inclusions (FOV is ~0.3
1417 mm), and: (d) Brightly illuminated close-up of (c), showing that this diamond is in
1418 fact transparent (FOV is ~0.3 mm).
1419

1420 Figure 15. Photomicrographs of Cempaka diamonds showing surface features and
1421 growth features: (a) partially resorbed diamond with pronounced negative crystal
1422 indents (3 mm); (b) pronounced dark brown radiation burns (2 mm); (c) large surface
1423 micro-disks (2mm), and; (d) zoning seen with polarized light (2 mm).
1424
1425 Figure 16. Histogram and cumulative frequency of relative diamond grain-size
1426 distribution from 8863 diamonds from the Cempaka paleoalluvium showing a
1427 multimodal grain size distribution. The data used to produce this plot are presented in
1428 Supplementary data table 5.
1429
1430 Figure 17. Schematic diagram of a continent-continent collision zone and the process
1431 by which diamonds associated with anhydrous UHP metamorphic rocks could be
1432 brought to the surface. This process was proposed as a primary source of the
1433 Cempaka diamonds due to their proximity to the Meratus-Bobaris ophiolites and
1434 Meratus Accretionary Complex. In reality, such a process would probably involve
1435 multiple tectonic mode switches driving phases of crustal extension and shortening as
1436 discussed by Lister and Forster (2009).
1437
1438

Figure 18. Map of the Sundaland region showing the distribution of major alluvial diamond deposits and districts. Alluvial diamonds in Sundaland are associated with Permian glacial marine diamictites. Kalimantan's diamonds are not likely to be derived from major fluvial systems reworking the Sundaland deposits and carrying these diamonds to Borneo as the Malayasian tin belt and Schwaner Mountains have been elevated regions since the Cretaceous and would have impeded any such drainage from the west (figure adapted from van Leeuwen, 2014).

Figure 19. (a) Map showing the present-day location of the Cempaka alluvial diamond deposit, the SW Borneo, East Java and Banda Embayment blocks as well as the location of various diamond deposits in northern and western Australia. (b) A rigid-plate reconstruction shows the current-day location of the Cempaka alluvial deposit rotated relative to an arbitrarily fixed Australian Plate and the possible transport direction of diamonds via major fluvial systems. This provides a maximum estimate of the transport distance between the Borneo terranes and Australian mainland as this reconstruction does not account for crustal extension in the NW Shelf. The Borneo fragments are rotated using the rotation poles of Hall (2012). Greater India is rotated relative to Australia as per White et al. (2013). The location of the Australian diamond deposits was taken from Jaques (2005).

Supplementary Data Captions

Supplementary Data Table 1: Results of spinel major element mineral chemistry obtained from EMP analyses

Supplementary Data Table 2: Results of SHRIMP U-Pb isotopic analyses of detrital zircon from the Cempaka alluvial deposit

Supplementary Data Table 3: Age results obtained from zircon fission-track analyses

Supplementary Data Table 4: Zircon trace element chemistry obtained from LA-ICPMS analyses

Supplementary Data Table 5: Size distribution data of diamonds from the Cempaka alluvium

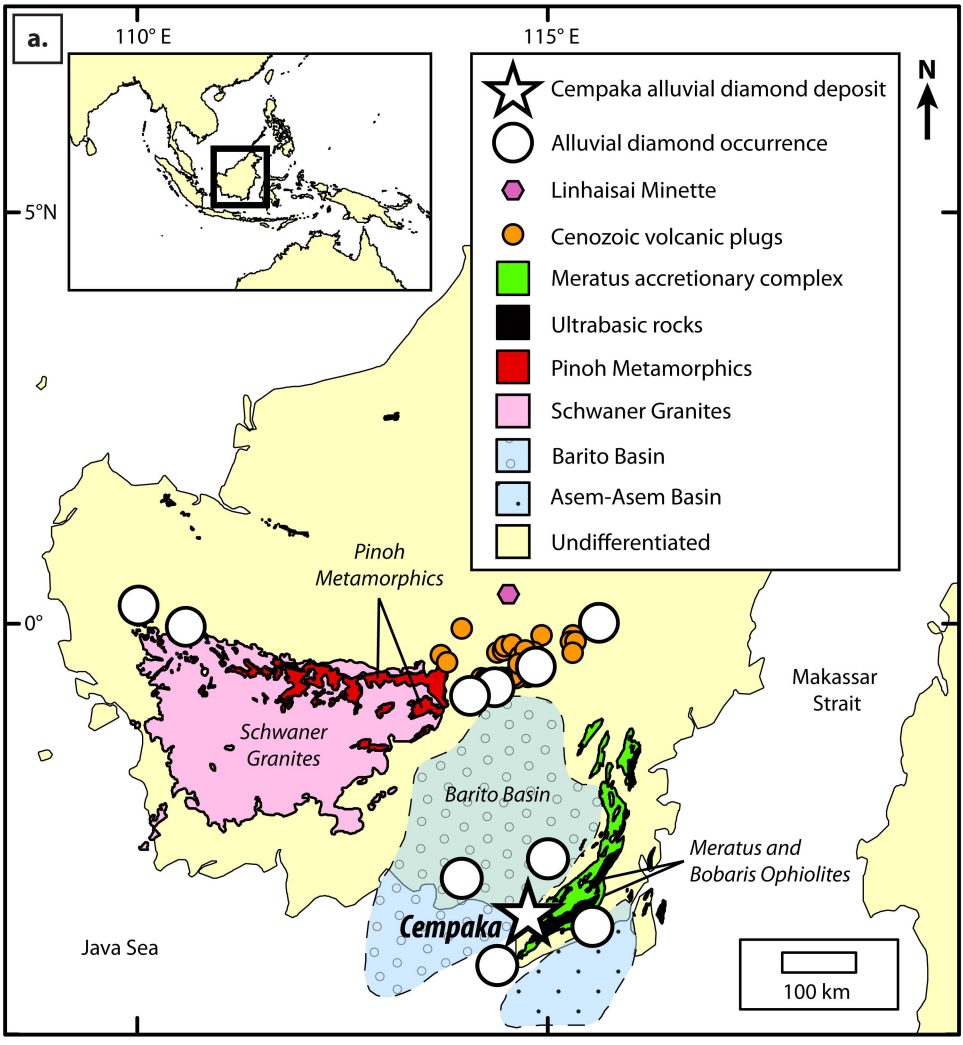
a.
110° E
115° E
5°N
0°
N
Cempaka alluvial diamond deposit
Alluvial diamond occurrence
Linhaisai Minette
Cenozoic volcanic plugs
Meratus accretionary complex
Ultrabasic rocks
Pinoh Metamorphics
Schwaner Granites
Barito Basin
Asem-Asem Basin
Undifferentiated
Pinoh Metamorphics
Schwaner Granites
Barito Basin
Meratus and Bobaris Ophiolites
Cempaka
Makassar Strait
Java Sea
100 km


b.

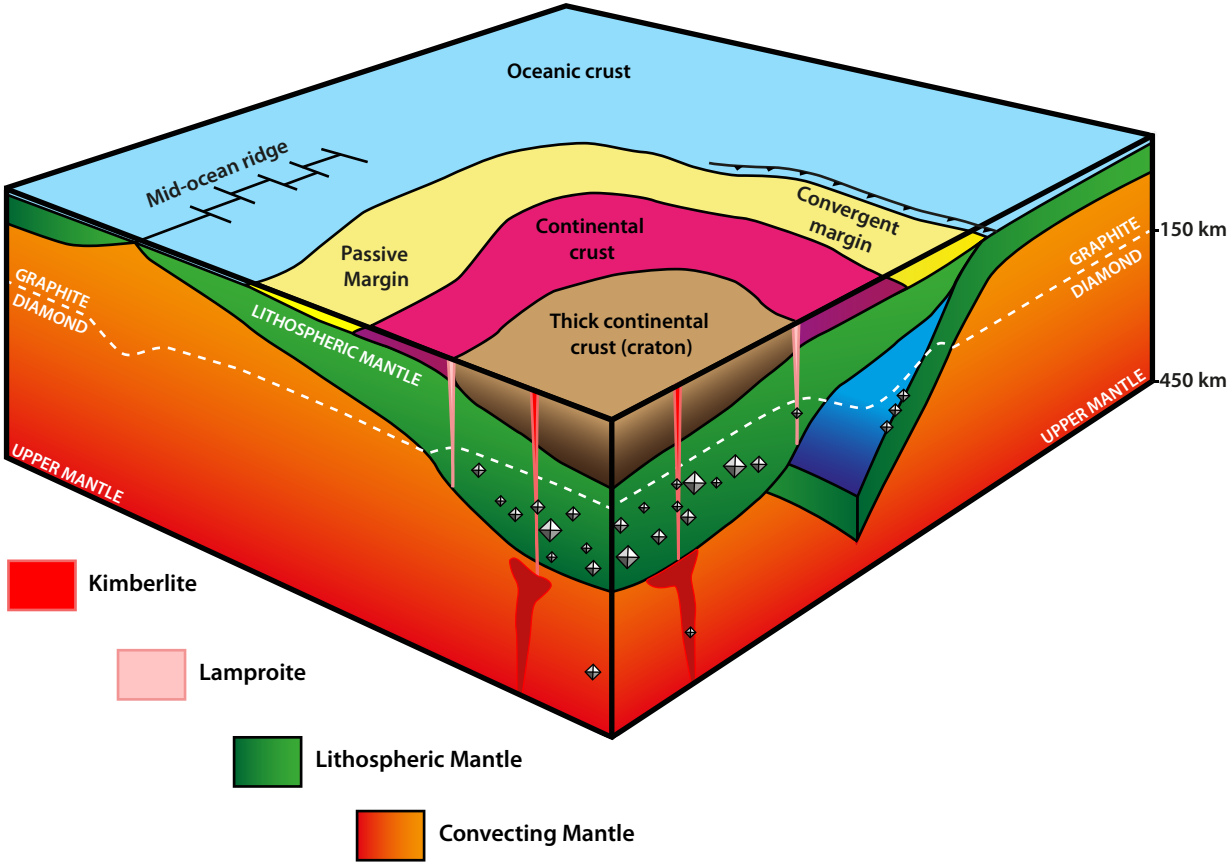
Oceanic crust
Mid-ocean ridge
Passive Margin
Continental crust
Convergent margin
Thick continental crust (craton)
GRAPHITE
DIAMOND
LITHOSPHERIC MANTLE
UPPER MANTLE
150 km
450 km
Kimberlite
Lamproite
Lithospheric Mantle
Convecting Mantle

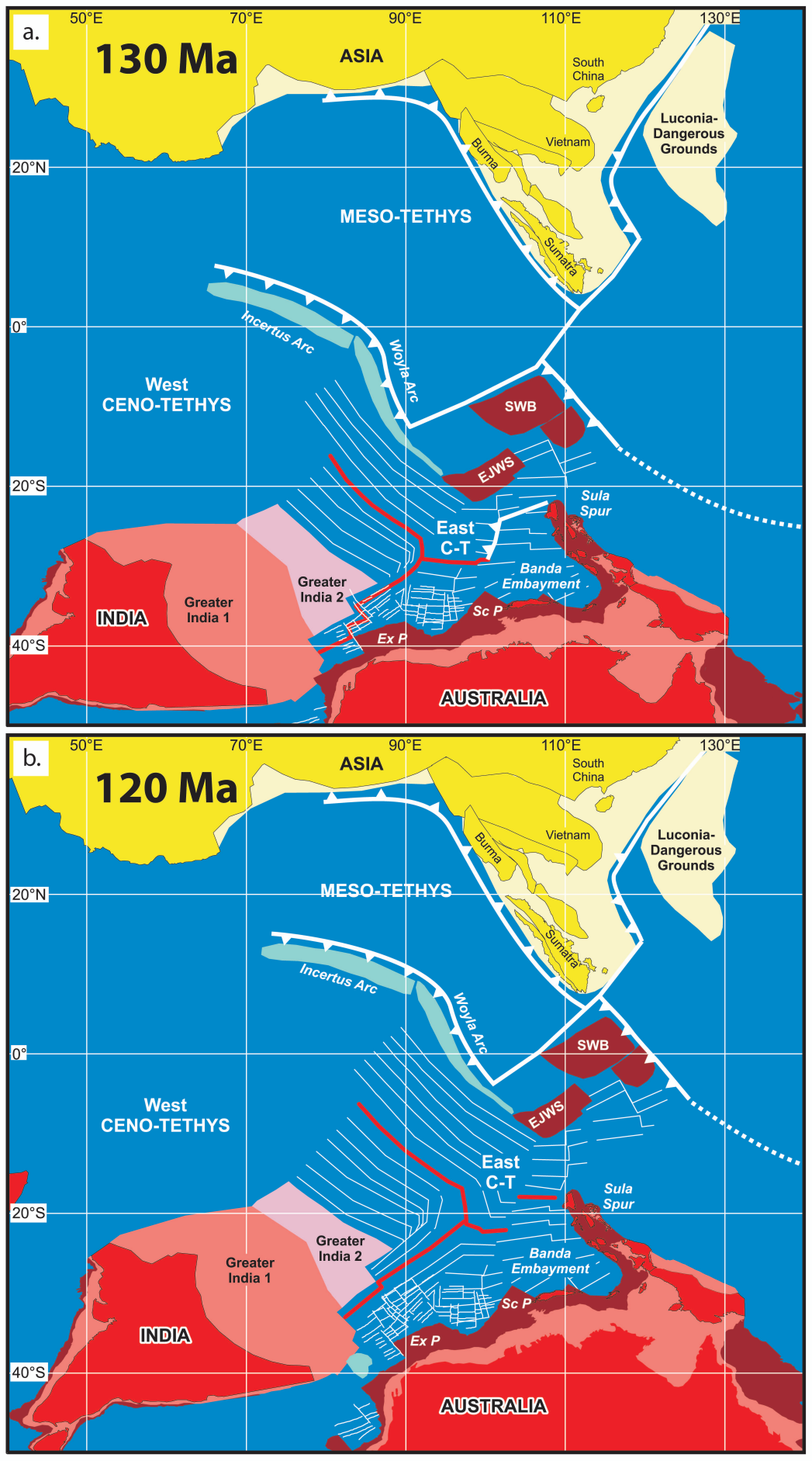
a.
130 Ma
50°E
70°E
90°E
110°E
130°E
ASIA
South China
Luconia-Dangerous Grounds
Vietnam
Burma
Sumatra
20°N
MESO-TETHYS
Incertus Arc
Woyla Arc
0°
West CENO-TETHYS
SWB
EJWS
20°S
Sula Spur
East C-T
Banda Embayment
Greater India 2
Greater India 1
INDIA
Sc P
Ex P
40°S
AUSTRALIA
b.
120 Ma
50°E
70°E
90°E
110°E
130°E
ASIA
South China
Luconia-Dangerous Grounds
Vietnam
Burma
Sumatra
20°N
MESO-TETHYS
Incertus Arc
Woyla Arc
0°
SWB
EJWS
West CENO-TETHYS
East C-T
Sula Spur
20°S
Greater India 2
Greater India 1
Banda Embayment
INDIA
Sc P
Ex P
40°S
AUSTRALIA

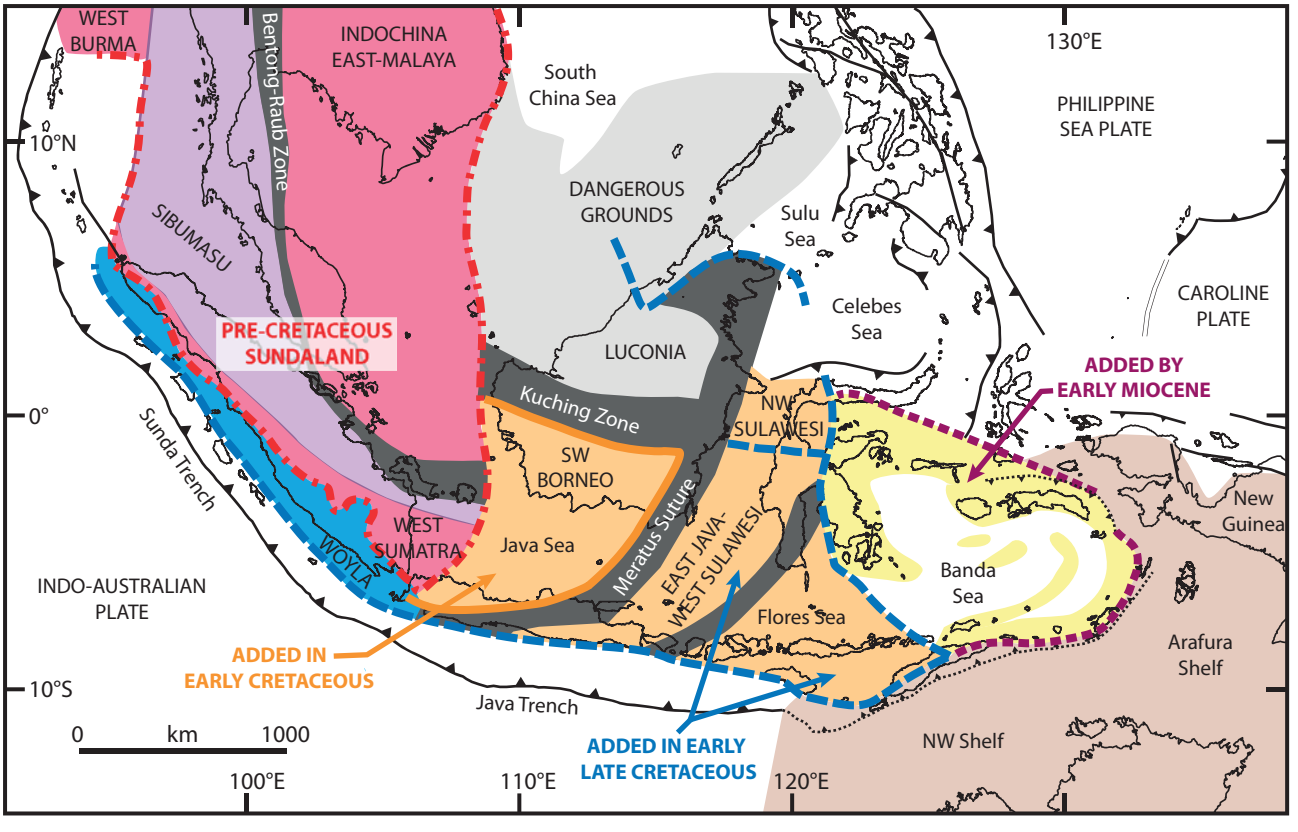

Derived from Gondwana in the Devonian

Derived from Gondwana in the Early Permian

Derived from Gondwana in the Late Jurassic

Mixture of crust accreted to Asian margin between the Triassic and early Late Cretaceous

Pre-Cretaceous Sundaland

Added to Sundaland in Early Cretaceous

Volcanic arc accreted in the Cretaceous

Suture Zone

Banda Arc and Fragmented Sula Spur

Australian Continental Crust

Added to Sundaland in early Late Cretaceous

Added by Early Miocene

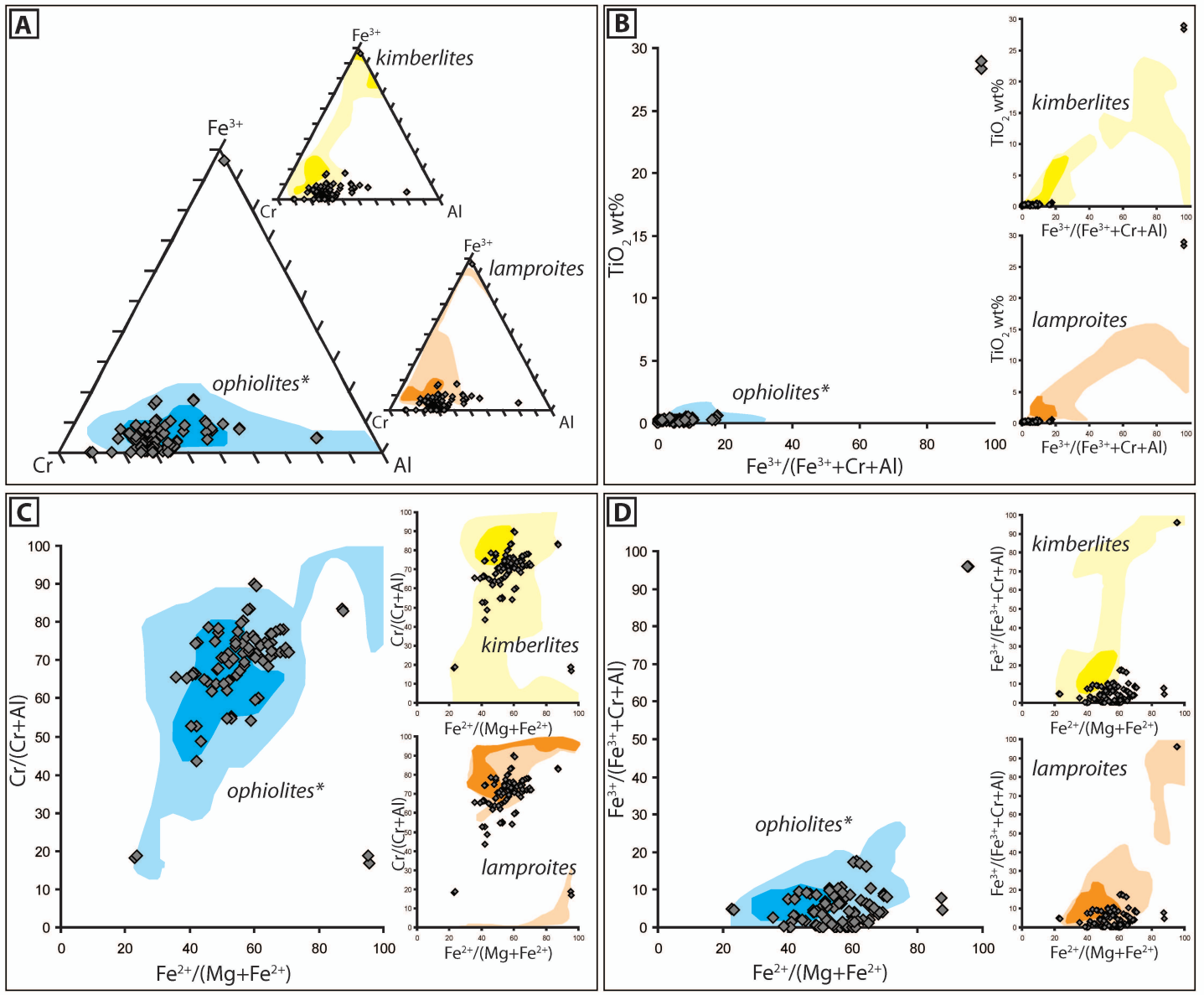
A
Fe3+
kimberlites
Cr
Al
Fe3+
lamproites
Cr
Al
Fe3+
ophiolites*
Cr
Al
B
TiO2 wt%
ophiolites*
Fe3+/(Fe3++Cr+Al)
kimberlites
TiO2 wt%
Fe3+/(Fe3++Cr+Al)
lamproites
TiO2 wt%
Fe3+/(Fe3++Cr+Al)
C
Cr/(Cr+Al)
ophiolites*
Fe2+/(Mg+Fe2+)
kimberlites
Cr/(Cr+Al)
Fe2+/(Mg+Fe2+)
lamproites
Cr/(Cr+Al)
Fe2+/(Mg+Fe2+)
D
Fe3+/(Fe3++Cr+Al)
ophiolites*
Fe2+/(Mg+Fe2+)
kimberlites
Fe3+/(Fe3++Cr+Al)
Fe2+/(Mg+Fe2+)
lamproites
Fe3+/(Fe3++Cr+Al)
Fe2+/(Mg+Fe2+)

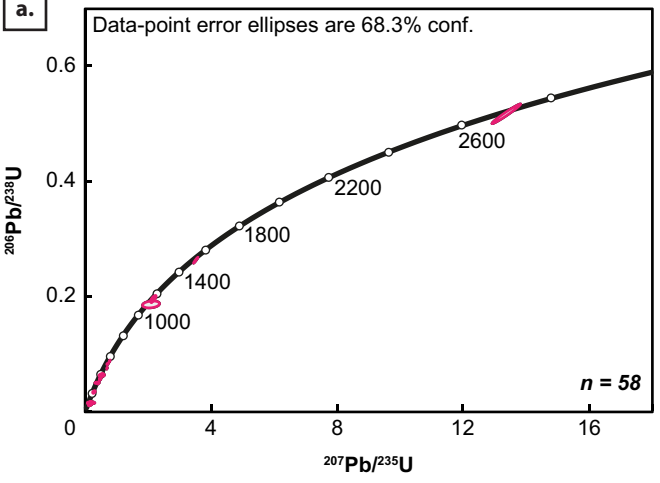
a.
Data-point error ellipses are 68.3% conf.
0.6
0.4
0.2
0
4
8
12
16
2600
2200
1800
1400
1000
n = 58
206Pb/238U
207Pb/235U

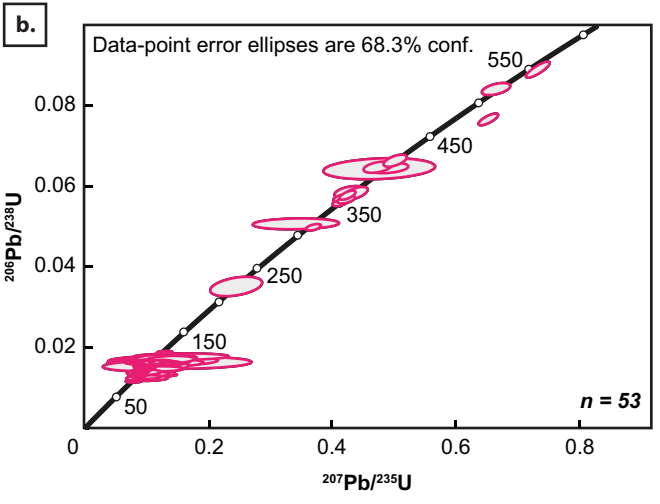
b.
Data-point error ellipses are 68.3% conf.
0.08
0.06
0.04
0.02
0
0.2
0.4
0.6
0.8
550
450
350
250
150
50
n = 53
206Pb/238U
207Pb/235U

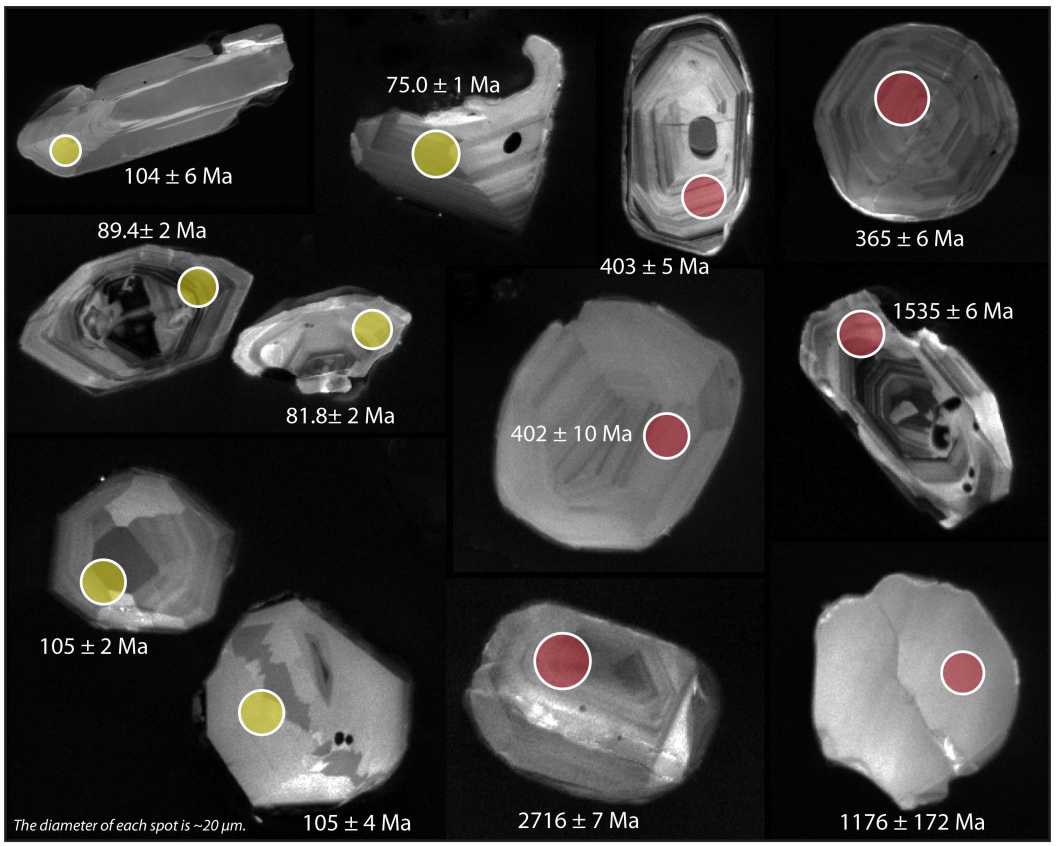
104 ± 6 Ma
75.0 ± 1 Ma
403 ± 5 Ma
365 ± 6 Ma
89.4± 2 Ma
81.8± 2 Ma
1535 ± 6 Ma
402 ± 10 Ma
105 ± 2 Ma
105 ± 4 Ma
2716 ± 7 Ma
1176 ± 172 Ma
The diameter of each spot is ~20 µm.

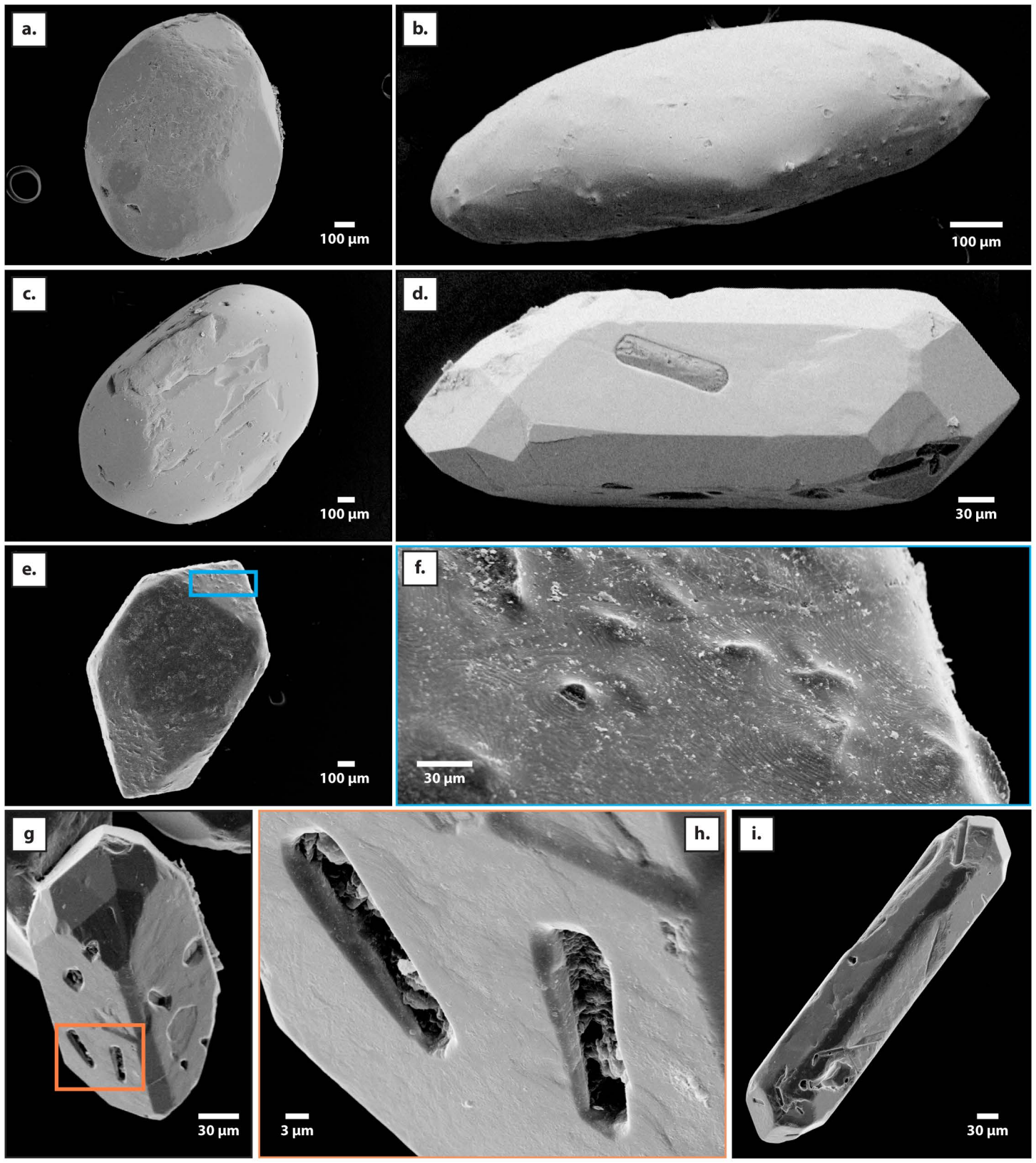
a.
100 µm
b.
100 µm
c.
100 µm
d.
30 µm
e.
100 µm
f.
30 µm
g
30 µm
h.
3 µm
i.
30 µm

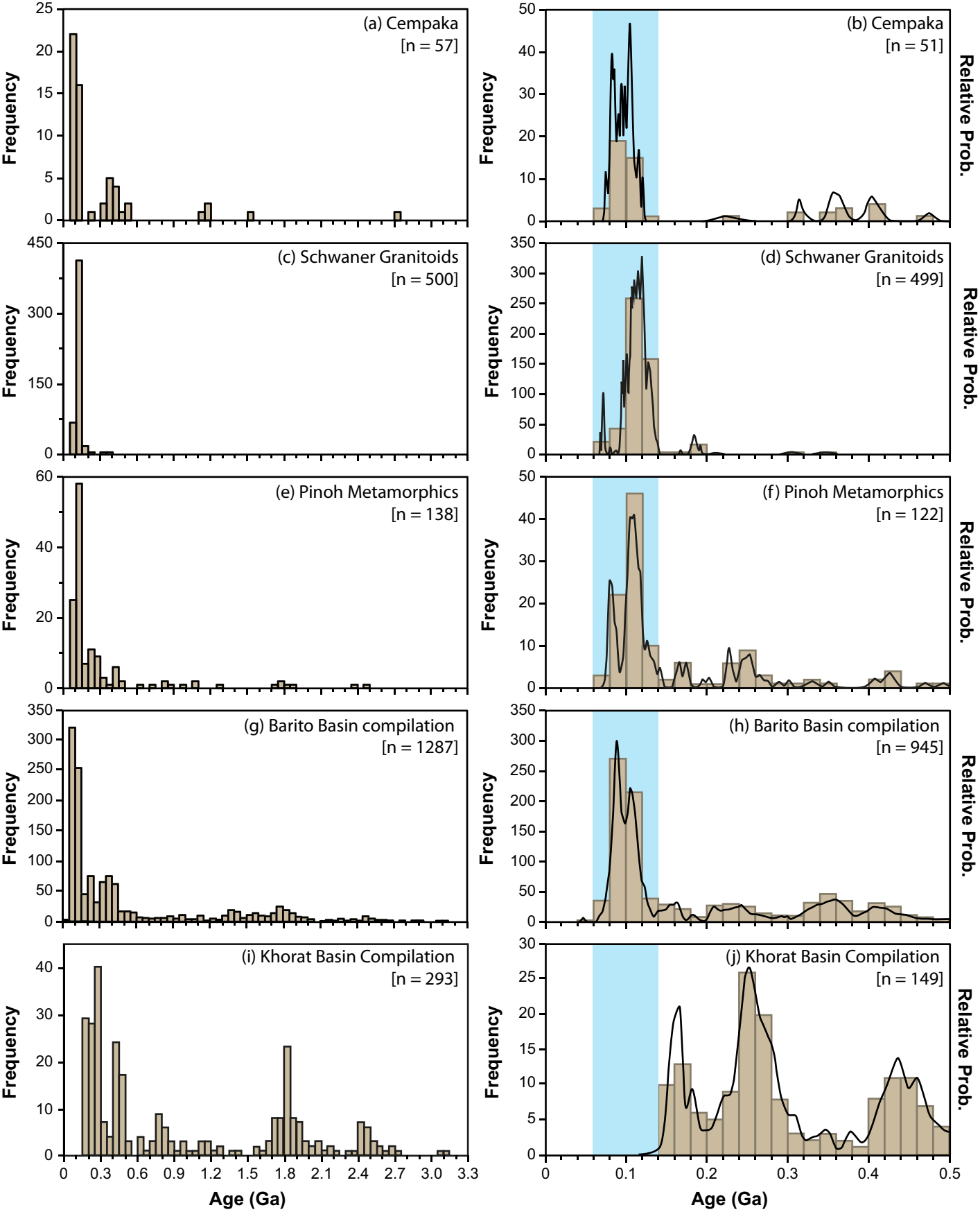
(a) Cempaka
[n = 57]
(b) Cempaka
[n = 51]
(c) Schwaner Granitoids
[n = 500]
(d) Schwaner Granitoids
[n = 499]
(e) Pinoh Metamorphics
[n = 138]
(f) Pinoh Metamorphics
[n = 122]
(g) Barito Basin compilation
[n = 1287]
(h) Barito Basin compilation
[n = 945]
(i) Khorat Basin Compilation
[n = 293]
(j) Khorat Basin Compilation
[n = 149]
Frequency
Relative Prob.
Age (Ga)

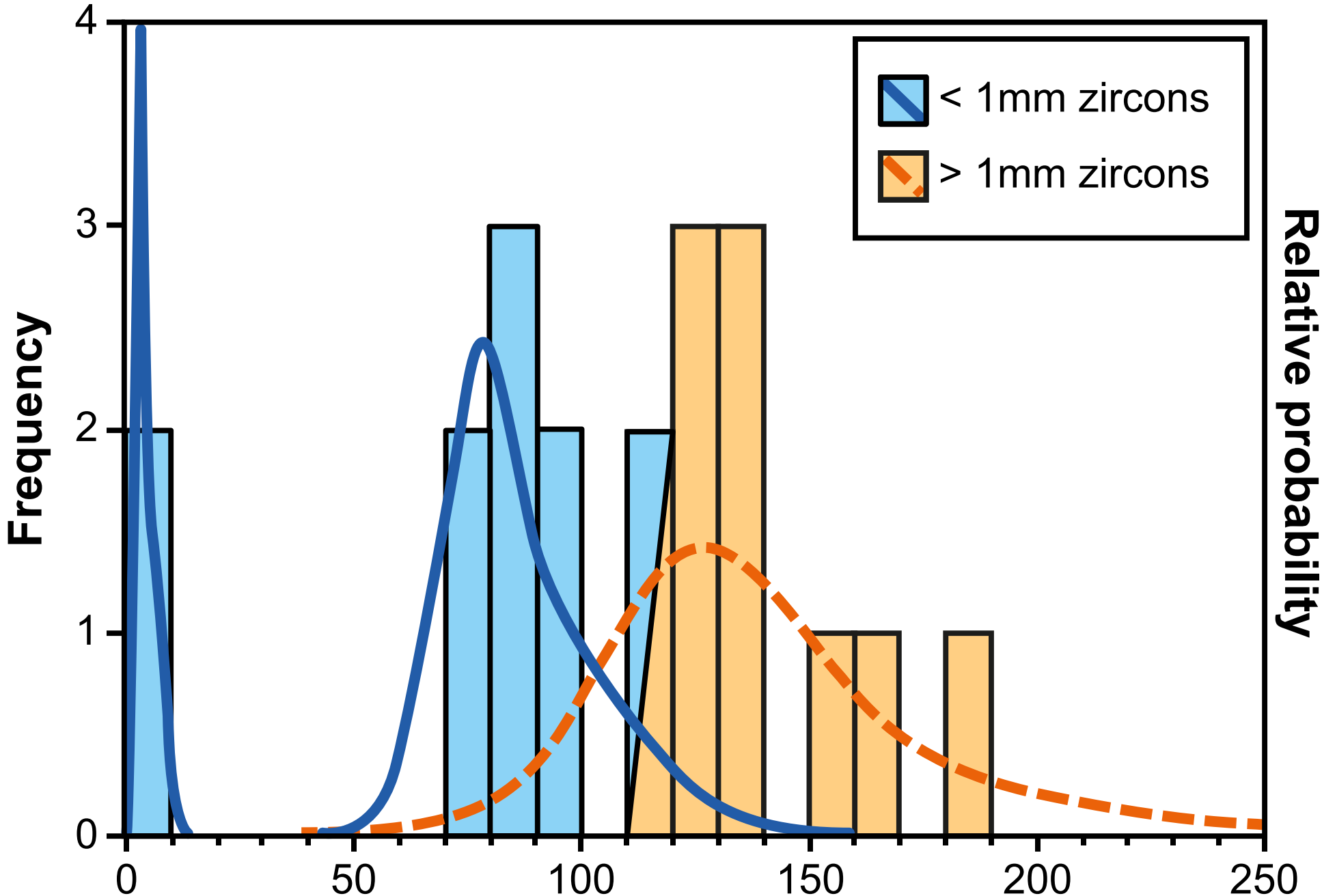
< 1mm zircons
> 1mm zircons
Frequency
Relative probability
0
1
2
3
4
0
50
100
150
200
250

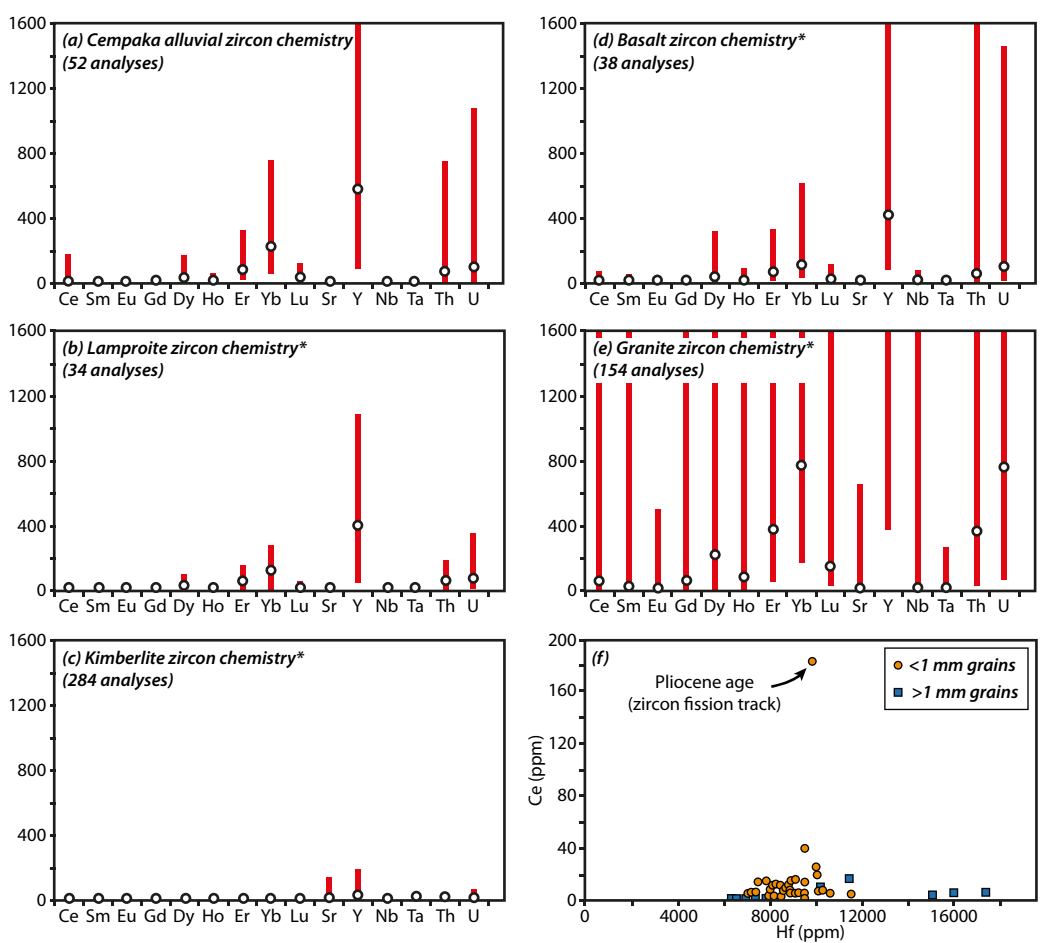
(a) Cempaka alluvial zircon chemistry
(52 analyses)
(d) Basalt zircon chemistry*
(38 analyses)
(b) Lamproite zircon chemistry*
(34 analyses)
(e) Granite zircon chemistry*
(154 analyses)
(c) Kimberlite zircon chemistry*
(284 analyses)
(f)
Pliocene age
(zircon fission track)
<1 mm grains
>1 mm grains
Ce (ppm)
Hf (ppm)
0
400
800
1200
1600
4000
8000
12000
16000
40
80
120
160
200
Ce Sm Eu Gd Dy Ho Er Yb Lu Sr Y Nb Ta Th U

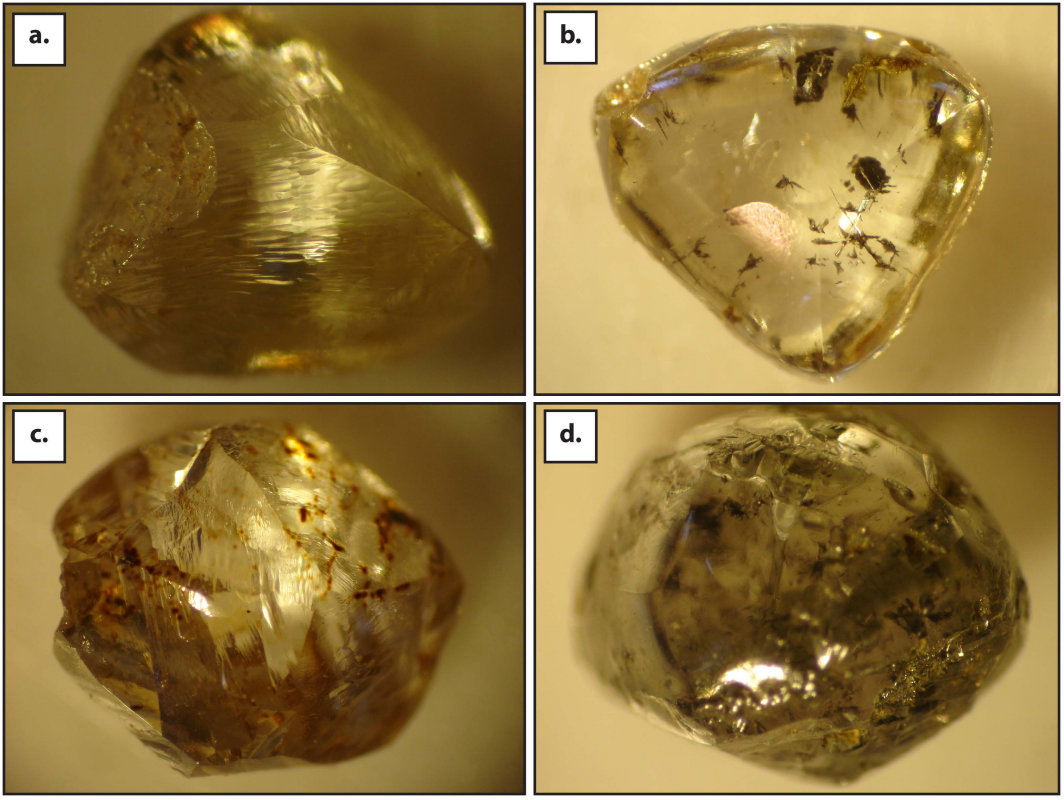
a.
b.
c.
d.

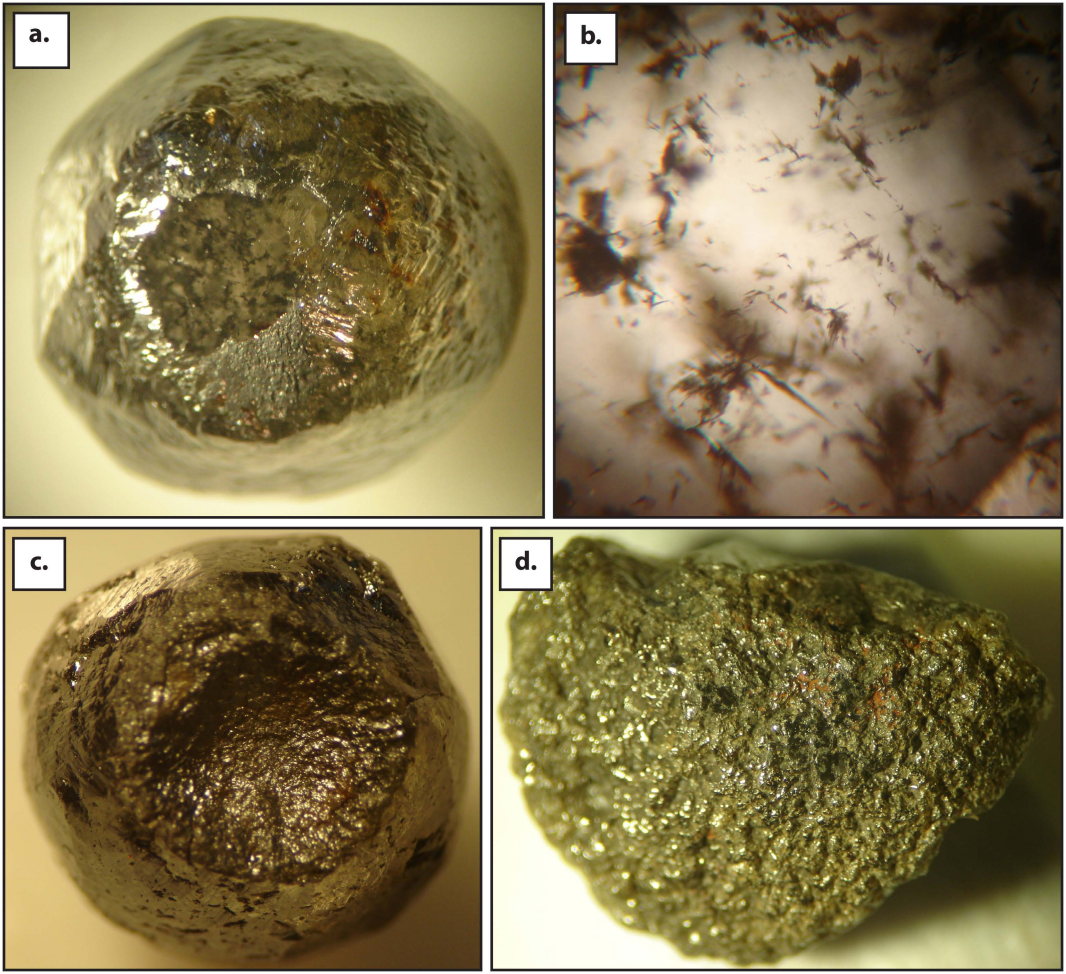
a.
b.
c.
d.

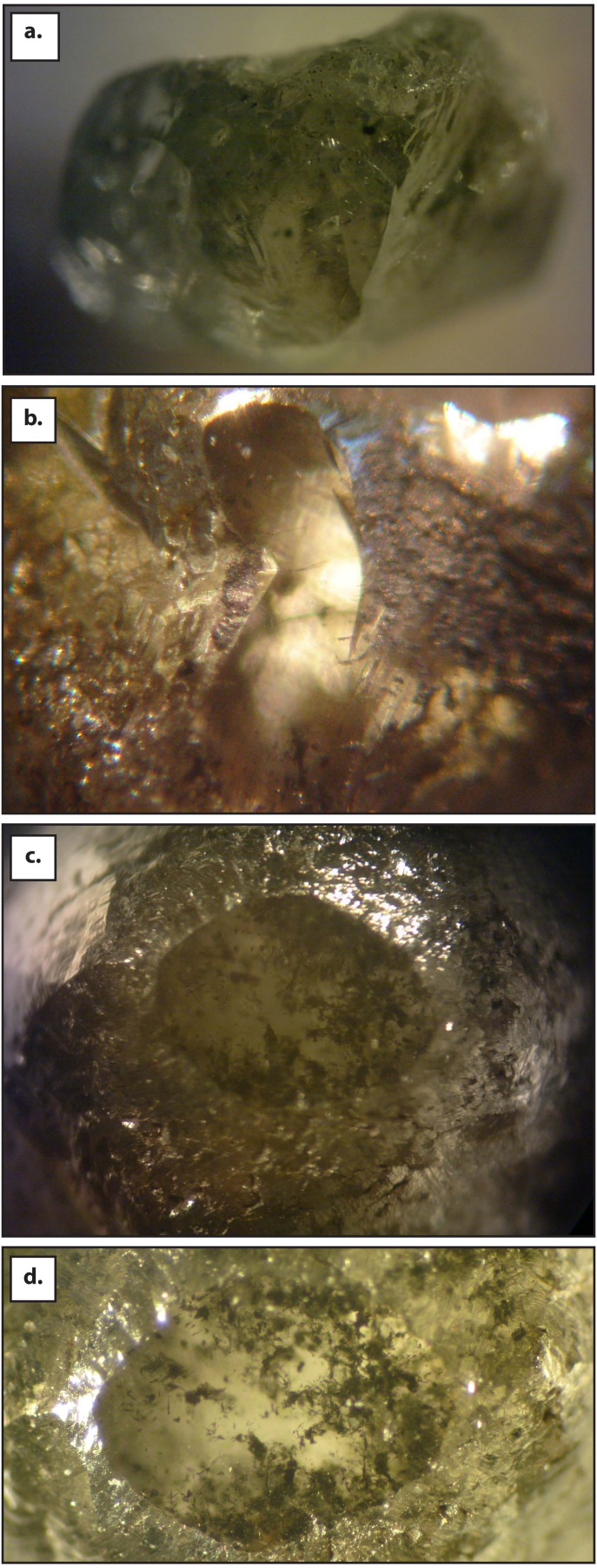
a.
b.
c.
d.

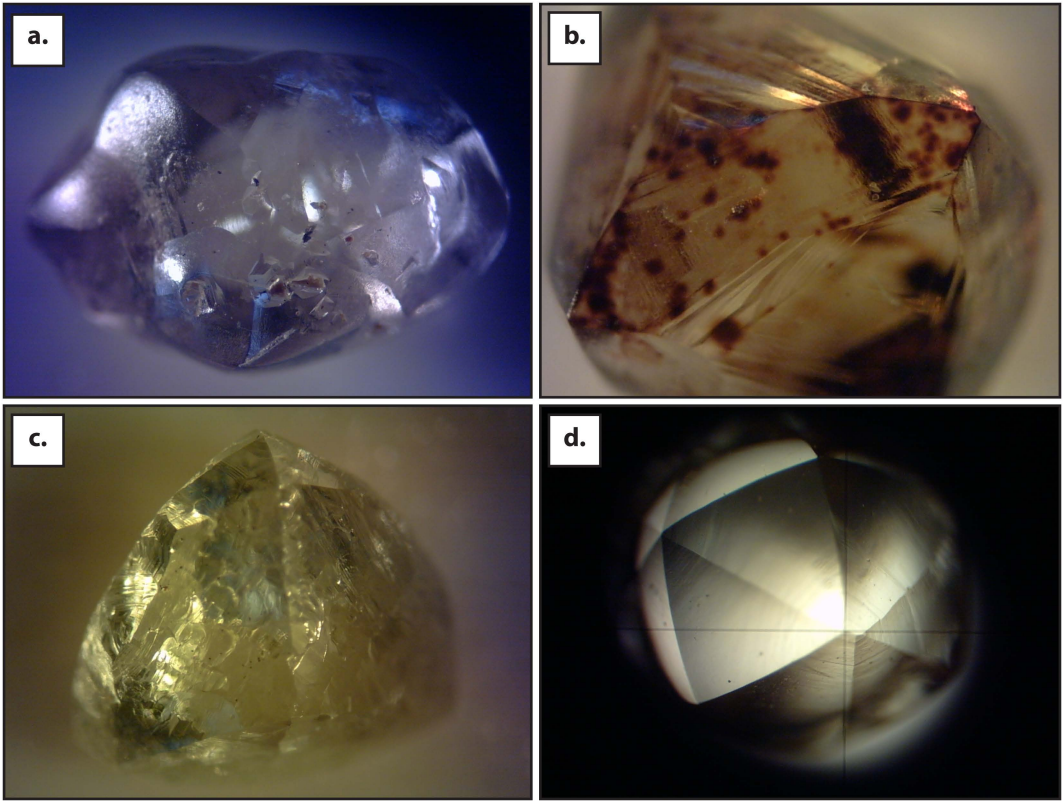
a.
b.
c.
d.

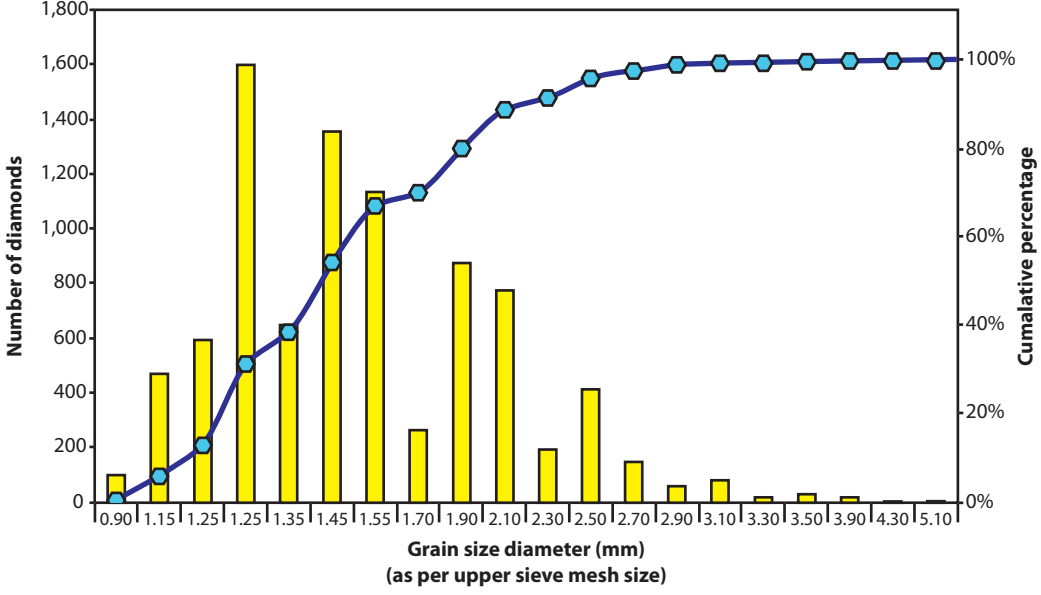
1,800
1,600
1,400
1,200
1,000
800
600
400
200
0
Number of diamonds
100%
80%
60%
40%
20%
0%
Cumalative percentage
0.90
1.15
1.25
1.25
1.35
1.45
1.55
1.70
1.90
2.10
2.30
2.50
2.70
2.90
3.10
3.30
3.50
3.90
4.30
5.10
Grain size diameter (mm)
(as per upper sieve mesh size)

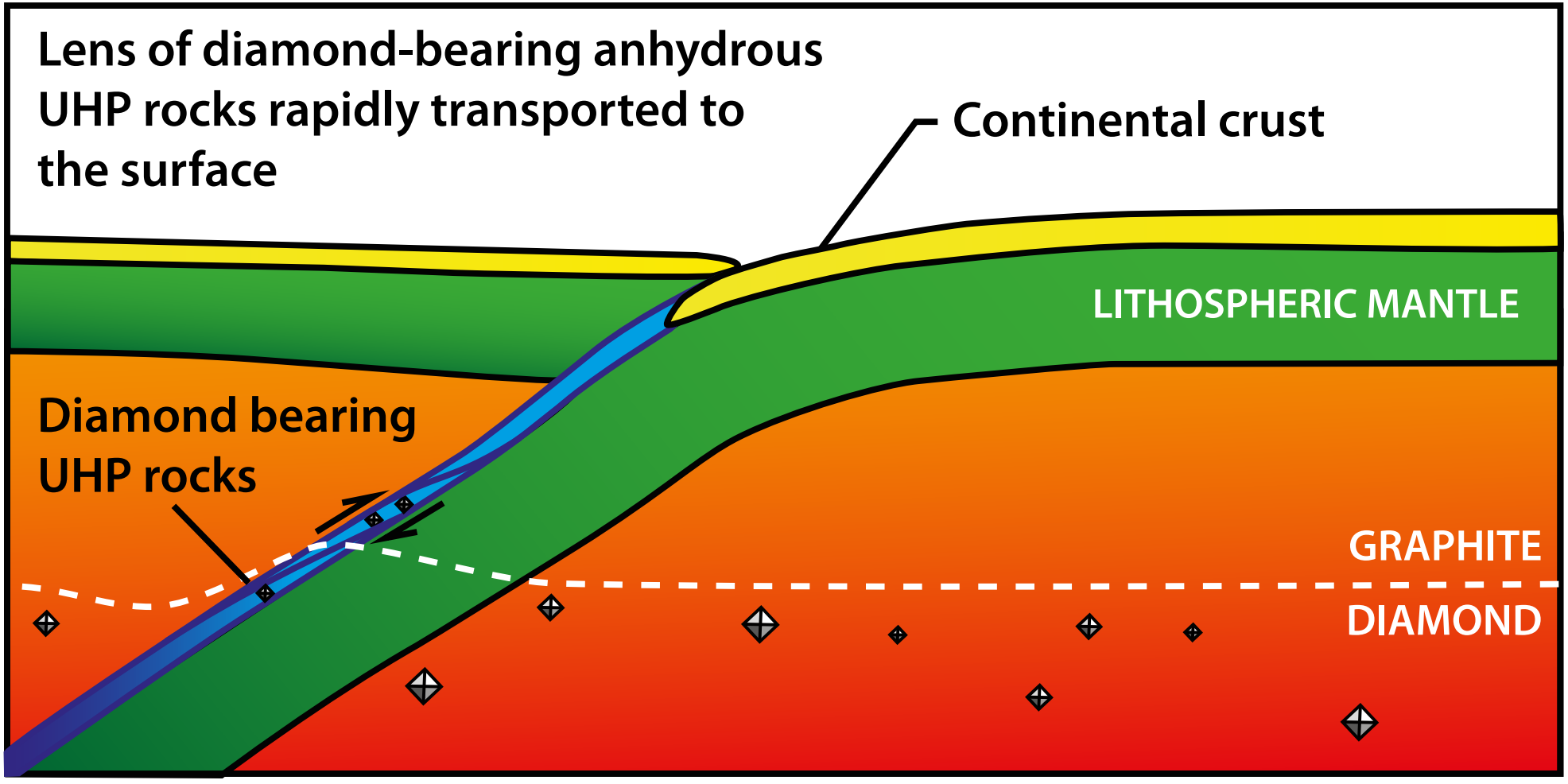
Lens of diamond-bearing anhydrous UHP rocks rapidly transported to the surface
Continental crust
LITHOSPHERIC MANTLE
Diamond bearing UHP rocks
GRAPHITE
DIAMOND

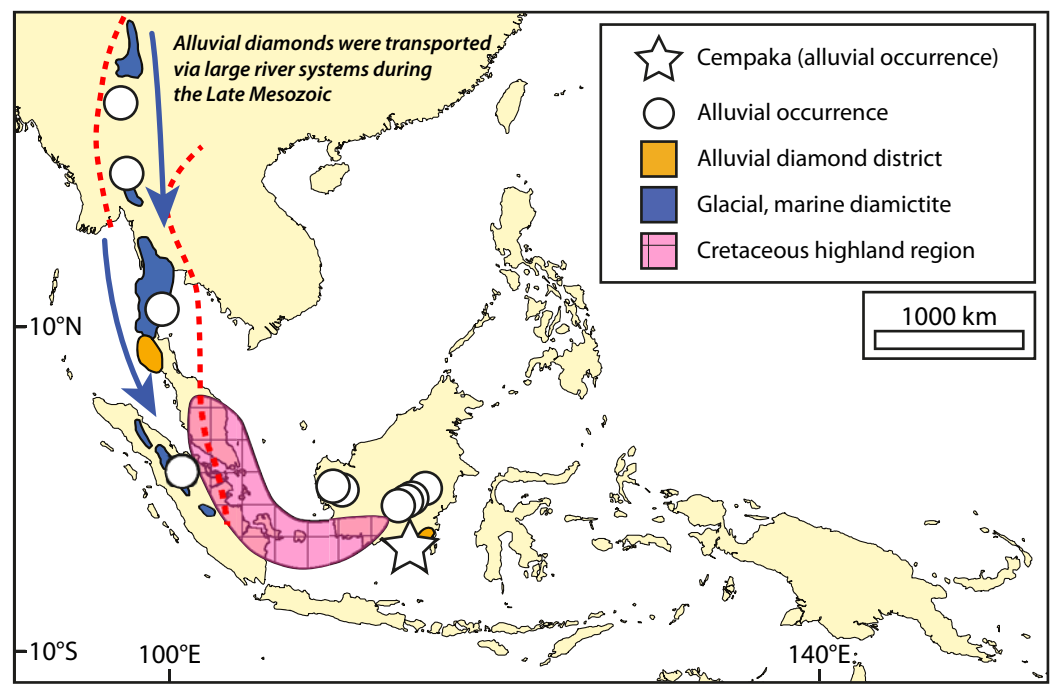
Alluvial diamonds were transported via large river systems during the Late Mesozoic
Cempaka (alluvial occurrence)
Alluvial occurrence
Alluvial diamond district
Glacial, marine diamictite
Cretaceous highland region
1000 km
10°N
10°S
100°E
140°E

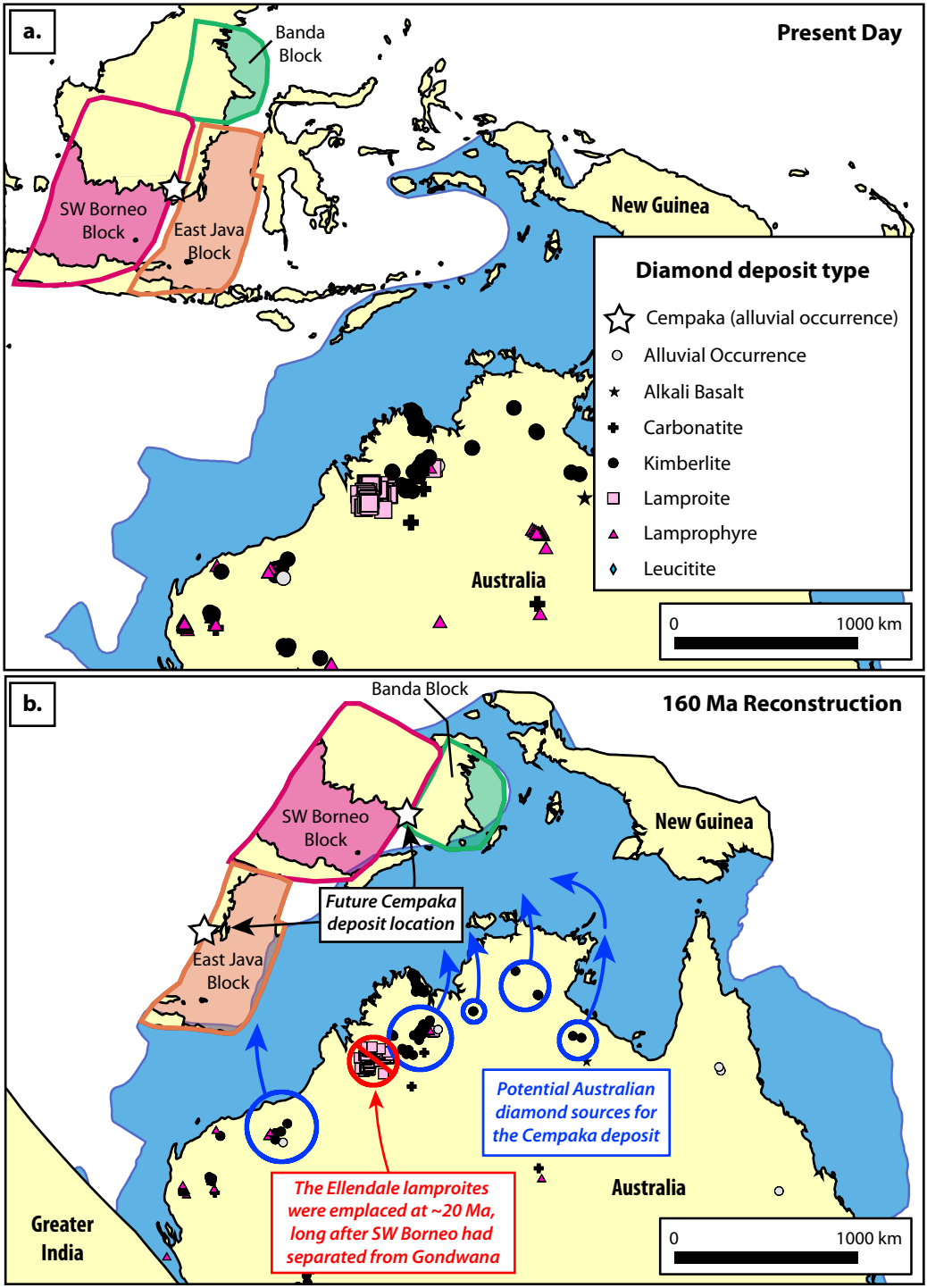
a.
Present Day
Banda Block
SW Borneo Block
East Java Block
New Guinea
Australia
Diamond deposit type
Cempaka (alluvial occurrence)
Alluvial Occurrence
Alkali Basalt
Carbonatite
Kimberlite
Lamproite
Lamprophyre
Leucitite
0
1000 km
b.
160 Ma Reconstruction
Banda Block
SW Borneo Block
East Java Block
New Guinea
Future Cempaka deposit location
Potential Australian diamond sources for the Cempaka deposit
The Ellendale lamproites were emplaced at ~20 Ma, long after SW Borneo had separated from Gondwana
Australia
Greater India
0
1000 km